测绘出版社 SURVEYING AND MAPPING PRESS

Remote Sensing and Forest Carbon Monitoring—a Review of Recent Progress, Challenges and Opportunities

Chengquan HUANG[1], Weishu GONG[1], Yong PANG[2]

1. *Department of Geographical Sciences*, *University of Maryland*, *Maryland* 20742, *USA*; 2. *Institute of Forest Resource Information Techniques*, *Chinese Academy of Forestry*, *Beijing* 100091, *China*

Abstract: Remote sensing provides key inputs to a wide range of models and methods developed for quantifying forest carbon. In particular, carbon inventory methods recommended by IPCC require biomass data and a suite of forest disturbance products. Significant progress has been made in deriving these products by leveraging publicly available remote sensing assets, including observations acquired by the legendary Landsat mission and new systems launched within the past decade, including Sentinel-2, Sentinel-1, GEDI, and ICESAT-2. With the L-band NISAR and P-band BIOMASS missions to be launched in 2023, the Earth's land surfaces will be imaged by optical and multi-band (including C-, L-, and P-bands) radar systems that can provide global, sub-weekly observations at sub-hectare spatial resolutions for public use. Fine scale products derived from these observations will be crucial for developing monitoring, reporting, and verification (MRV) capabilities needed to support carbon trade, REDD+, and other market-driven tools aimed at achieving climate mitigation goals through forest management at all levels. Following a brief discussion of the roles of forests in the global carbon cycle and the wide range of models and methods available for evaluating forest carbon dynamics, this paper provides an overview of recent progress and forthcoming opportunities in using remote sensing to map forest structure and biomass, detect forest disturbances, determine disturbance attribution, quantify disturbance intensity, and estimate harvested timber volume. Advances in these research areas require large quantities of well—distributed reference data to calibrate remote sensing algorithms and to validate the derived products. In addition, two of the forest carbon pools-dead organic matter and soil carbon—are difficult to monitor using modern remote sensing capabilities. Carefully designed inventory programs are needed to collect the required reference data as well as the data needed to estimate dead organic matter and soil carbon.

Key words: carbon models; forest disturbance; growth; structure biomass

Citation: Chengquan HUANG, Weishu GONG, Yong PANG. Remote Sensing and Forest Carbon Monitoring—a Review of Recent Progress, Challenges and Opportunities[J]. Journal of Geodesy and Geoinformation Science, 2022, 5(2): 124-147. DOI:10.11947/j.JGGS.2022.0212.

1 Introduction

It has been well-established that rapidly-increasing greenhouse gases in the atmosphere have contributed to observed global warming since the mid-20th century[1-2]. Curbing this increasing trend has been a major goal of the international community since the adoption of the United Nations Framework Convention on Climate Change (UNFCCC) in 1992. Following the Paris Agreement signed in 2015 and the 2021 Conference of the Parties (COP 26), more than 100 countries/parties have pledged to achieve carbon neutrality by the second half of the 21st century[3]. Achieving this ambitious goal will require both reducing carbon emissions wherever possible and enhancing carbon sequestration by terrestrial and aquatic ecosystems.

With the ability to sequester and store carbon for decades to centuries in biomass or wood products, the forest provides high potential for carbon management designed to enhance carbon uptake by terrestrial ecosystems[4]. In particular, the

Received date: 2022-02-24; accepted date: 2022-05-07
First author: Chengquan HUANG
E-mail: cqhuang@ umd.edu

United Nations Collaborative Program on Reducing Emissions from Deforestation and Forest Degradation in Developing Countries (REDD+) offers a framework to help developing countries reduce emissions from deforestation and forest degradation while achieving sustainable management of forests and the conservation and enhancement of forest carbon stocks[5]. A transparent and cost-effective measurement, reporting, and verification (MRV) system is crucial for the successful implementation of REDD+ projects[6-7]. Such a system should provide methods for calculating carbon fluxes that may arise from forest change driven by disturbances, management activities, and forest growth[8-9]. These flux estimates provide a basis for determining carbon credits, which are critical to carbon trade and to other tools needed to implement forest-based climate mitigation initiatives[10-11].

Carbon dynamics are governed by many physical and biogeochemical processes. In general, remote sensing is not capable of directly measuring carbon in most ecosystem pools. Instead, complicated methods or models are needed to calculate the amount of carbon in different pools and the fluxes between those pools. However, remote sensing is crucial to the derivation of many of the datasets required by a wide range of carbon estimation methods. A number of new remote sensing systems launched in the most recent decade, along with their free-access data policies, have provided opportunities to greatly improve many data products needed to support forest carbon monitoring. The unprecedented spatial and temporal details as well as the wide range of sensing capabilities (optical, radar, and LiDAR) make it possible to generate products with spatial details, timeliness, and accuracy that can better support MRV at both local and regional/national levels for REDD+ or other projects aimed at achieving climate mitigation goals through forest management.

The main purpose of this study is to provide a review of recent progress in using the newly available, publicly accessible remote sensing assets to advance forest carbon monitoring. We will provide an overview of the roles of the forest in the global carbon cycle, review the methods that are available for deriving forest carbon estimates, and discuss recent progress in deriving key datasets required by carbon inventory methods recommended by IPCC using existing remote sensing assets as well as opportunities offered by two forthcoming radar missions to be launched in 2023.

2 Forest and the Global Carbon Cycle

The global carbon cycle includes an active natural carbon cycle that circulates carbon between the reservoirs of the atmosphere, ocean, and terrestrial biosphere, and anthropogenic perturbations that occur on top of the natural carbon cycle[12-13]. Anthropogenic perturbations are caused by emissions from fossil fuel use and land use change, which lead to increased atmospheric CO_2 concentration and carbon changes in both ocean and land. Global carbon research is mainly concerned with (1) carbon emissions resulting from fossil fuel combustion and oxidation from other industrial processes plus land-use change and other human activities on land, and (2) the partitioning of emitted carbon between the atmosphere, ocean, and land. One of its primary goals is to quantify the size of and fluxes between carbon pools in the atmosphere, land, and aquatic systems, and how these pools change under anthropogenic perturbations[14]. Recent studies show that current estimates of the global carbon budget are highly uncertain. For the decade of 2010—2019, for example, emissions from land use change and carbon uptake by land were estimated at 1.6 ± 0.7 GtC y^{-1} (gigaton carbon per year) and 3.4 ± 0.9 GtC y^{-1} respectively[15]. For the decade of 2007—2016, these estimates were 1.3 ± 0.7 GtC y^{-1} and 3.0 ± 0.8 GtC y^{-1} respectively, and the global budget had an imbalance of 0.6 GtC y^{-1}[16]. Reducing uncertainties of carbon budget estimates is crucial for accurate projections of future concentrations of CO_2 in the atmosphere and changes in the Earth's climate[17].

The forest plays complicated roles in many Earth system processes related to climate change, including surface energy fluxes, hydrological processes, and the carbon cycle[18-19]. While accounting for less than one one-third third of the total land area, forestland stores ~45% of terrestrial carbon and contributes ~50% of terrestrial net primary production[20]. It is estimated that forests absorb approximately one fourth of anthropogenic CO_2 emissions and store over 80% of aboveground carbon, which is more than any other terrestrial ecosystem[15]. Therefore, relatively minor alterations to carbon storage or cycling in forest ecosystems could have a substantial impact on atmospheric carbon dioxide concentrations. Improved quantification of forest carbon dynamics is crucial for reducing uncertainties in the global carbon budget.

Carbon in forestland is typically partitioned into soil and biomass pools (Fig.1). Live biomass is further partitioned into aboveground and belowground biomass, while dead biomass, which releases carbon gradually through decay, includes litter, standing dead, and coarse woody debris[21]. Forest carbon dynamics are governed in large part by disturbance and regrowth[22]. Vegetation growth provides a mechanism for transferring atmospheric carbon to the forest ecosystem. About half of the Gross Primary Production (GPP)—the initial uptake of carbon through photosynthesis—is used by plants for growth and maintenance. The remaining carbon contributes to the Net Primary Production (NPP). Net Ecosystem Production (NEP) is the difference between NPP and heterotrophic respiration (i.e., CO_2 emission by non-photosynthetic organisms)[4]. Over time, some carbon in live biomass may be removed or lost due to harvest/logging, fire, storm damage, or insect/disease outbreak, and the remaining carbon contributes to the Net Biome Production (NBP).

NBP is a critical parameter to consider for long-term carbon storage. It is a small fraction of GPP and can be positive or negative; at equilibrium it would be zero[23]. When trees are harvested, the harvested carbon can be used as biofuel to reduce emissions from fossil fuel use, or stored in wood products where the carbon is released gradually over decades or longer[24]. Burying the used wood products will keep the remaining carbon in those products from being released into the atmosphere for even longer[25].

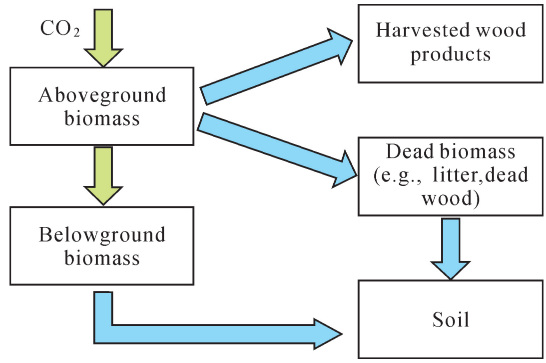

Fig. 1 A conceptual diagram of carbon uptake through vegetation growth (green arrows) and carbon transfer (blue arrows) among major pools of forest ecosystems. Carbon can be released from each pool through abrupt (e.g., fire) or gradual (e.g., decay) processes. An inventory of forest carbon dynamics can be derived by summing up carbon changes in all pools (see Section 3.4)

A major goal of forest carbon management is to increase carbon sequestration and storage by forests and related carbon pools (e.g., wood products) while reducing and/or delaying carbon release from those pools[26-27]. A suite of forestry-related climate change mitigation strategies has been proposed, including afforestation, reforestation, forest management, reduced deforestation, harvested wood product management, and use of forestry products for bioenergy to replace fossil fuel use, among others[2]. These strategies are key elements of major climate initiatives, including the Kyoto Protocol, REDD+, and the Paris Agreement[5, 28]. Implementing these strategies requires robust carbon accounting systems to provide reliable estimates of carbon credits for carbon trade and to support the Measurement, Reporting, and Verification (MRV) of carbon pools and fluxes[4, 29-30].

3 Forest Carbon Estimation Approaches

Terrestrial carbon fluxes can be estimated using top-down models or bottom-up approaches, which have also been used together to constrain global carbon estimates[31-33]. Top-down methods are typically based on the inversion of atmospheric transport models constrained by atmospheric CO_2 measurements. Ocean and land fluxes are estimated based on the residuals left unexplained by fossil fuel emissions, which are assumed to be known[34]. Results from these models indicated that the terrestrial ecosystem has been a net carbon sink[35-37]. The sink estimates derived using the top-down approach differ substantially depending on the transport models used[31, 38]. Further, because the underlying transport models used by the top-down approach are primarily constrained by CO_2 movement in the atmosphere and not by any specific features of terrestrial ecosystems, it is not possible to attribute the sink estimates derived using this approach to fine scale forest or other ecosystems. The rest of this paper will mainly focus onthe bottom-up approach, which includes process-based models designed to represent ecosystem processes controlling carbon cycle dynamics, models that use accounting-based methods to track carbon fluxes arising from land use change, and methods that use forest inventory data. A combination of multiple models is often used in synthesis studies aimed at constraining the boundaries of carbon estimates for a given region.

3.1 Process-based models

A large number of models have been developed based on different principles of earth system processes to represent carbon transfer among different pools (Tab. 1). These models can be divided into two categories: diagnostic and prognostic[39]. Both model types use external data to provide climate forcing. Diagnostic models require satellites or other external sources to prescribe vegetation conditions and disturbance dynamics. These models are primarily used to estimate carbon fluxes under given vegetation conditions and disturbance history using algorithms of varying complexity. Example diagnostic models include BEPS[40], different variants of the CASA model[41-43], and ISAM[44].

Instead of requiring vegetation and disturbance history information prescribed using external data, prognostic models calculate vegetation dynamics based on succession and other ecological theories. They can be used for diagnostic analyses and for predicting future carbon dynamics under different climate change and management scenarios. However, because they are much less constrained by observations than diagnostic models, they may produce carbon estimates that are more variable (and likely less reliable) than diagnostic models. Example prognostic models include Can-IBIS[45], CLM-CN[46], DLEM[47], LPJ-wsl[48], ORCHIDEE[49], SiB3[50], and TEM[51].

Tab.1 A partial list of process-based models for carbon studies (based on Literatures [39] and [52])

Model name	Developers/References
BEPS	Chen et al.[40]; Ju et al.[53]
Biome-BGC	Bond-Lamberty et al.[54]
Can-IBIS	Foley et al.[45]; Kucharik et al.[55]
CASA	Randerson et al.[43]
CASA GFEDv2	van der Werf et al.[41, 42]
CENTURY	Parton et al.[56]
CLM-CASA	Randerson et al.[57]
CLM-CN	Thornton et al.[46]; Randerson et al.[57]
DLEM	Tian et al.[47]
DNDC	Li et al.[58]
ED	Hurtt et al.[59]; Moorcroft et al.[60]
EDCM	Liu et al.[61]
FIRE-BGC	Keane et al.[62]
FORCLIM	Bugmann[63]
FOREST-BGC	Running and Gower[64]
FVS	Dixon[65]
HYBRID	Friend et al.[66]
InTEC	Chen et al.[67]
ISAM	Jain and Yang[44]
LANDIS	Mladenoff[68]
LINKAGES	Pastor and Post[69]
LPJ-wsl	Sitch et al.[48]; Bondeau et al.[70]
ORCHIDEE	Krinner et al.[49]
SiB3	Baker et al.[50]
SORTIE	Pacala et al.[71]
TEM	Raich et al.[51]; McGuire et al.[72]

Depending on the modeling structures used, process-based models can also be grouped as compartment models or ecosystem demography models[52]. In compartment models, the carbon pools of a stand are typically organized by leaves, branches, stems, roots, and other biomass compartments. Most of these models can simulate forest growth and recovery under the influence of climate and atmospheric (CO_2 and nitrogen) changes, as well as the interaction between growth variation and heterotrophic respiration variation, although they do not necessarily represent tree diameter, height, density, or other structural variables explicitly. Therefore, they are especially valuable for understanding how forest carbon processes are affected by climate change[73-74]. The generalized approach to understanding ecosystem carbon dynamics provided by these models has been examined extensively. They have been used in many studies to simulate biogeochemical processes of forests associated with disturbance[75-76].

Ecosystem demography models, also known as gap models, are built upon the notion that a forest stand is a composite of many horizontally homogeneous patches that have different species compositions, ages, and/or successional stages[77]. This modeling strategy provides a mechanism to represent the impact of disturbances on forest composition and structure, making it possible to simulate the establishment, growth, and mortality of mixed-species and mixed-age forests[74, 78]. Example gap models include SORTIE[71], FIRE-BGC[62], LINKAGES[69], FORCLIM[63], HYBRID[66] LANDIS[68], FVS[65], and ED[59-60]. These models can simulate the impacts of management practices, disturbances, and climate change on the long-term dynamics of forest structure, biomass, and species composition[79-80]

3.2 Accounting-based methods

Accounting provides an alternative approach to tracking carbon fluxes arising from land use change[81-82]. One of the most widely used accounting-based methods is a bookkeeping model developed by Houghton[83-84]. This model keeps track of carbon in four major pools: live aboveground and belowground biomass; dead biomass, including coarse woody debris; harvested wood products; and soil organic carbon. It calculates carbon changes arising from four change types related to forestland, including forest disturbance by fire, industrial wood harvest, conversion from forest to cropland, and conversion from forest to urban land[21]. It has been used to derive carbon estimates from historical land use change across the globe[21, 84-85] and for many countries and regions, including the US[86], China[87], and the Brazilian Amazon[88]. Together with remote sensing-based forest change and biomass products, bookkeeping models have been used to estimate carbon fluxes due to deforestation in recent decades[89-92].

Largely following the bookkeeping approach of the Houghton Bookkeeping model, Hansis et al. developed the Bookkeeping for Land Use Emission (BLUE) model[93]. Unlike the original Houghton Bookkeeping model, however, BLUE is spatially explicit—it runs on a grid of half-degree cells, and can track the carbon fluxes caused by each year's events through time. Other forms of accounting-based models have also been developed and/or used to produce flux estimates for historical land use change[94-98].

The original Houghton Bookkeeping model uses ecozones as its modeling units, and hence can only produce estimates with a minimum geographical unit at the ecozone level. While such estimates are valuable for understanding carbon dynamics at a regional, national and global scale, they lack critical spatial details needed to support carbon management decision-making by local authorities and individual land owners. The same can be said of the results produced by the BLUE model with a half-degree cell size[93]. To address this limitation, two modified bookkeeping models have been developed independently based on the Houghton Bookkeeping model. One is a spatially explicit bookkeeping model developed by Tang et al., which has been used to produce land use-driven carbon estimates at 30- to 500-m resolutions[99-100]. The other is a grid-based carbon accounting model developed by Gong et al., which has been used to produce flux estimates driven by forest change at the 30-m resolution[127].

3.3 Inventory-based methods

For countries or regions that have forest inventory programs designed to produce periodic inventory of their forest resources[101-102], the inventory data collected through those programs are highly valuable for deriving forest carbon estimates. The Forest Inventory and Analysis (FIA) program of the US Forest Service, for example, has a network of more than 100,000 plots distributed across the country where trees are measured at 5- to 10-year intervals[102-103]. These tree measurements can be converted to growing stock and biomass carbon using allometric equations and volume-to-carbon conversion coefficients[104-105].

FIA data has been used as a primary data source to estimate forest carbon dynamics at state, regional, and national levels for the US[106-110]. Similar studies have been reported for other countries or regions, including Canada[111], Russia[112], and Europe[113-114].

Given that forest inventory programs typically collect measurements over large numbers of plots selected using design-based sampling schemes, inventory data can provide comprehensive regional estimates of carbon fluxes for aboveground carbon with relatively small errors. Such estimates may serve as references for evaluating process-based models, which typically have much larger uncertainties[39]. However, there is no long-term, comprehensive monitoring data for soil and litter/deadwood at regional to national scales. Carbon estimates for these pools are typically estimated using empirical models developed based on limited data collected over small study regions, and hence may have much larger uncertainties than those for the biomass pool. The Forest Health Monitoring (FHM) program of the US Forest Service has partially implemented carbon monitoring for soil and litter/deadwood. This program requires that additional information on soil, forest floor and down woody debris be collected for a subset (~8000) of the FIA plots[115]. When remeasurements for a sufficient number of plots become available, uncertainties in the estimates derived using inventory-based methods should be greatly reduced.

3.4 Synthesis and good practice approaches

Each of the carbon calculation methods discussed above has its own strengths and limitations. In particular, process-based models tend to produce estimates with larger uncertainties than inventory-based methods, partly because process-based models can differ in terms of the processes included, the types of algorithms employed to represent those processes, and the choices of input data. Large discrepancies existed among estimates derived using more than a dozen process-based models over North America[39]. In order to better constrain the boundaries of carbon estimates, most carbon studies use multiple methods to derive flux estimates at regional to global scales. For example, Bastos et al. used a top-down approach and a total of 16 land surface models to evaluate the impact of the 2015/2016 El Niño on the terrestrial carbon cycle[31]. Ťupek et al. compared an inventory-based method with three process-based models to evaluate forest carbon fluxes over Europe[116]. Hayes et al. combined results derived using top-down approaches, inventory data, and a suite of diagnostic and prognostic models to reconcile the contemporary carbon balance over North America[33]. Many estimates of the global budget were derived by synthesizing results derived using multiple methods[15-16].

Given the large number of available carbon calculation methods and the various issues they have, IPCC developed comprehensive guidelines for national greenhouse gas inventories, which will be referred to as the IPCC Guideline hereafter[8]. Over a land area, the net flux (ΔC) is calculated as the sum of carbon changes in aboveground biomass (ΔC_{AB}), belowground biomass (ΔC_{BB}), dead organic matter (ΔC_{DOM}, including litter and dead wood), Harvested Wood Products (ΔC_{HWP}), and soil (ΔC_{soil}) (Fig.1)

$$\Delta C=\Delta C_{AB}+\Delta C_{BB}+\Delta C_{\mathrm{DOM}}+\Delta C_{\mathrm{HWP}}+\Delta C_{\mathrm{soil}}$$

To accommodate the different levels of technical readiness of different countries, a three-tiered approach is provided for estimating these quantities. Tier 1 methods are the simplest to use, with equations and default parameter values (e.g., emission and stock change factors) readily available from the IPCC Guideline book. The same methodological approach is used in Tier 2. Where available, however, country-or region-specific data should be used, which in general should be more appropriate for the climatic regions, land-use systems, and livestock categories in the study region. Often, higher temporal and spatial resolutions and more disaggregated activity data are also used in Tier 2. In Tier 3, higher order methods that can provide estimates of greater certainty than lower tiers are used. These include models and inventory measurement systems tailored to address national circumstances, repeated over time, driven by high-resolution activity data, and disaggregated at a sub-national level.

Based on the IPCC Guideline, many countries developed comprehensive carbon inventory methods and datasets, including the US[117], Canada[118], Australia[119], and European countries[120]. Because good inventory data in general can provide more accurate estimates, they are used frequently when available. For example, the forest carbon accounting framework of the US is fundamentally driven by the annual forest inventory conducted by the FIA program. Many developing countries, however, may need additional help in order to follow the IPCC Guideline to develop their own carbon inventory capabilities[121].

4 Opportunities from Remote Sensing

With the ability to cover all land areas of the Earth's surface in a relatively short time, satellite remote sensing has become indispensable for carbon studies. Remote sensing observations have been used to derive many quantities/variables related to various carbon pools and/or processes, including vegetation status, vegetation dynamics, ecosystem fluxes, soil properties, meteorological variables, and atmospheric carbon (Tab. 2). Comprehensive reviews of efforts dedicated to the retrieval of these properties using remote sensing technology over multiple decades have been provided in Literatures [14] and [122]. Progress in the remote sensing of specific surface properties or variable groups has also been discussed in Literatures [123]—[126].

Despite the large array of methods available for deriving carbon estimates, quantification of forest carbon dynamics remains challenging. Currently, most process-based models can only produce carbon estimates with large uncertainties at coarse spatial resolutions or for very large regions. They are not mature enough for use in MRV systems needed to support REDD+ or other forest-related climate mitigation programs or initiatives. The inventory-based methods, though they may produce more accurate estimates, can only be used by countries/regions that have good inventory data. The good practice approaches recommended by the IPCC are flexible enough to be used by all countries. When implemented using fine spatial grids, these methods could produce flux estimates with critical spatial details needed to calculate carbon credits and support carbon management at local or individual land owner levels[99-100, 127].

Tab.2 A partial list of variables/parameters important for estimating forest carbon dynamics that may be derivable using remote sensing technology

General category	Variable list
Plant characteristics	Foliar nitrogen, chlorophyll, lignin concentration, leaf area, leaf water content, stress/drought
Vegetation status	Stand age, species composition, canopy cover, height, volume, biomass
Vegetation dynamics	Land cover/use change, disturbance, management, harvested wood products, growth rates
Ecosystem fluxes	SIF, GPP, NPP, NEP, NBP/NEE, FAPAR, ER
Soil properties	Soil moisture, nutrient, soil organic carbon
Meteorological variables	Precipitation, temperature (including LST), ET, VPD, PAR
Atmospheric carbon	CO_2, CH_4

For terrestrial ecosystems, carbon accounting is concerned with carbon changes in five pools: aboveground biomass, belowground biomass, dead organic matter, soil, and harvested wood products. Fluxes between these pools are estimated directly or indirectly based on biomass and forest disturbance data (Tab.3). The sections below examine opportunities offered by existing and forthcoming remote sensing capabilities for mapping aboveground biomass and a suite of variables related to forest change, including the location, timing, type/causality, and intensity of forest disturbance as well as harvested wood products.

4.1 Relevant remote sensing capabilities

Landsat has been the primary system for monitoring the Earth's surface with sub-hectare details for much of the decades dating back to the 1970s[128-129], which will continue with the successful launch of Landsat 9 in 2021. A number of systems launched during the past decade greatly enhanced this monitoring capability, including two Sentinel-2 satellites, two Sentinel-1 satellites, the ICESAT-2 Satellite, and the Global Ecosystem Dynamics Investigation (GEDI) mission. Although there are many other optical and SAR missions that can support forest carbon monitoring[130-131], these are the major missions designed with the intent of achieving wall-to-wall imaging or comprehensive sampling of all land areas of the globe. Following the free-data policy of the Landsat established in 2008[132], observations acquired by these missions are freely available for public use, making it possible to produce carbon estimates for any region of the globe at a relatively low cost. Sentinel-2 observations are highly comparable to Landsat data[133]. Sentinel-1 provides C-band radar data systematically acquired across the globe on a quasi-ten-day basis[134]. GEDI and ICESAT-2 provide dense samples of LiDAR-based vegetation structure measurements that have footprint sizes comparable to those of Landsat and Sentinel data and are well distributed across the globe[135-136].

Tab.3 General methods and input data required for estimating major carbon pools of terrestrial ecosystems (based on IPCC[8])

Carbon pools	Estimation methods/input data
Aboveground biomass	Ground measurements, remote sensing, land use/disturbance
Belowground biomass	No change, or modeled based on aboveground biomass
Dead organic matter	No change, or modeled based on land use/disturbance data
Soil	No change, or modeled based on land use/disturbance data
Harvested wood products	FAO database, survey data, remote sensing based

4.2 Forest structure and biomass mapping

Aboveground biomass is one of the most valuable products for carbon studies, because it can be directly related to landscape carbon, and can provide a constraint for both growth models and the calculation of emissions from disturbance[137-138]. It is also often used to estimate carbon in belowground biomass and dead organic matter, which are difficult to derive directly using remote sensing observations. Of the three remote sensing instrument types—optical, radar, and LiDAR, LiDAR can provide metrics that are directly related to forest structure and height[139-140], and hence has the best potential for biomass estimation[141-142]. Methods have been developed for identifying individual trees using high density point cloud LiDAR data[143-144]. Vegetation species information could also be used to improve LiDAR-based biomass estimation[145]. However, current spaceborne LiDAR systems, including ICESAT-2 and GEDI, can only collect samples along their tracks. These samples need to be used together with wall-to-wall observations to create spatially contiguous map products. Approaches like the Field-Airborne-Spaceborne (FAS) method developed by Pang et al. are often used to integrate field measurements, airborne LiDAR data, and satellite imagery to create biomass maps[146-147].

In general, radar is more sensitive to vegetation structure than optical systems. While radar offers promise for predicting forest biomass and for mapping general forest types and tree species in floristically simple landscapes[148-151], radar signal saturates at mid- to high-biomass levels, with the location of the saturation point being wavelength dependent[150, 152-161]. Although optical remote sensing data may not be as sensitive to forest structure and biomass as LiDAR and radar data[162-163], they have proved to be useful for mapping forest biomass over large areas. For example, texture information derived from high resolution imagery was found useful for estimating biomass[164]. Landsat-based biomass products have been developed for selected areas in the US[165], interior Alaska[166], Canadian boreal forests[167], and the conterminous US[168-169]. Field data and/or LiDAR measurements from the ICESAT-1 mission have been used to calibrate MODIS observations to develop biomass maps for the US[169-171], China[172-173], tropical Africa[174], and tropical regions over multiple continents[175]. Similarly, a 30-m biomass map has been developed for China based on Landsat spectral data and ALOS/PALSAR radar imagery calibrated using field inventory data and ICESAT-1 forest height estimates[176].

Given the large quantities of LiDAR samples being collected by ICESAT-2 and GEDI, these samples will allow for more robust calibration/validation of mapping algorithms at regional to global scales[177].

Efforts have been made to establish models for estimating biomass from GEDI metrics[178]. GEDI/ICESAT-2 measurements are being used with observations from Landsat and other missions to improve biomass mapping in an ever-growing number of studies[179-182]. Since LiDAR metrics are directly related to several structural attributes, including canopy cover and a suite of height metrics, they can be used together with optical and/or radar images to map those attributes. For example, LiDAR samples have been used to calibrate Landsat time series data to map forest height[183-184]. The dense and globally-distributed LiDAR samples collected by GEDI were crucial to the development of a global 30-m tree height map[185]. GEDI measurements have also been used together with VIIRS observations to produce a suite of forest structure attributes for CONUS, including canopy cover, height, plant area index, and height diversity index[186]. Height and other structural variables have been used to reduce uncertainties in biomass modeling or to produce biomass estimates directly based on allometric equations[187-188].

4.3 Forest disturbance monitoring

With its first satellite launched in 1972, the Landsat mission has produced a fine resolution imagery record of the Earth's surface for half a century. Landsat data has been used to map land cover and various surface characteristics in numerous studies[128-129]. The multi-decadal time series observations provided by Landsat are especially valuable for understanding the carbon dynamics related to land use change. Since 2003, Goward and colleagues have led efforts to characterize US forest disturbances using time series Landsat observations[22, 189-192]. These studies became known as the North American Forest Dynamics (NAFD) study, which has been identified as a core project of the North American Carbon Program. Major NAFD products include forest disturbances mapped at an annual time step[193], which were derived using the Vegetation Change Tracker (VCT) algorithm and a 30-year surface reflectance record[194]. VCT detects anomalous events in the per-pixel spectral time series caused by forest disturbances, including harvest/logging, fire, storm damages, and insect outbreaks[190]. VCT disturbance products have been validated through many studies[190-192, 194-197].

In addition to the NAFD products, several other geospatial datasets have been developed to provide information on specific disturbance types at national or sub-national scales. In particular, the Monitoring Trends in Burn Severity (MTBS) project[198], a collaboration between the US Forest Service and USGS, has mapped the extent and severity of large fires across the United States using ground-based fire records and Landsat images acquired from 1984 to present. The US Forest Service has been producing Aerial Detection Survey (ADS) sketch maps recording the location (polygons) of insect outbreaks, which can be used to produce consolidated data products on insect-related mortality[199-200]. Hurricane and tornado tracks have been recorded by NOAA as early as 1851. Combining these tracks with wind models allows for the assessment of wind damages from tropical storms[201].

During the past decade or so, many other algorithms designed for detecting forest change using time series Landsat data emerged, including LandTrendr[202-203], continuous change detection and classification (CCDC)[204], composite2change (C2C)[205-206], Exponentially Weighted Moving Average Change Detection (EWMACD)[207], Vegetation Regeneration and Disturbance Estimates through Time (VRDET)[208], and Image Trends from Regression Analysis (ITRA)[209]. A comprehensive assessment over 6 regions selected from across the US showed that most of these algorithms had large commission and omission errors, although results with slightly better and more balanced accuracies could be derived by combining these algorithms using ensemble approaches[195]. Building on the CCDC algorithm, the USGS is developing an integrated approach for Land Change Monitoring, Assessment, and Projection (LCMAP)[210], which is intended to map land cover and change on an annual basis[211]. Globally, forest changes have been mapped based on multi-temporal tree cover products[212- 213]

With radar becoming increasingly more

available and affordable, radar time series observations have been used to derive forest change products. Many studies demonstrated the feasibility of using radar data together with time series Landsat observations to map forest disturbance[214-217], recovery[218], and biomass dynamics[219-221]. Launched in 2014 and 2016, the pair of Sentinel-1 satellites have produced a global archive of dense time series radar observations unaffected by cloud or solar illumination conditions. These observations have revisit intervals of 12 days or less for most of the land areas of the globe, making it possible to map forest harvest on a monthly basis[222]. When produced on a near-realtime basis, such monthly forest change maps can serve as alert products that can be used by local authorities to halt or intervene with deforestation activities as those activities are happening[223].

4.4 Other disturbance attributes

Most disturbance mapping algorithms focus on identifying the location and timing of forest disturbances. The carbon fluxes arising from those disturbances are affected by disturbance type or attribution, disturbance intensity, as well as carbon influx to harvested wood products. Some progress has been made in deriving these products. Schroeder et al. demonstrated that fire and clearcut harvest could be separated using Landsat time series data[224]. Zhao et al. used support vector machines to identify the causality of disturbances mapped by VCT[225]. Schroeder et al. developed an approach for mapping six disturbance types based on the shape of the temporal profiles of time series Landsat data[226]. Building on the NAFD disturbance products, Schleeweis et al. mapped forest disturbance types/causal agents across the conterminous U. S. (CONUS) from 1986 to 2010[227]. Time series-based methods have also been developed for mapping disturbance attribution for Canadian forests[228-229].

Many disturbance mapping algorithms use spectral change (SC) indices to detect disturbance events. These indices represent the spectral manifestation of the impact of the detected events, and therefore might be indicative of the severity of those events. For example, Huang et al. grouped disturbance pixels into four intensity levels based on a change magnitude calculated using the integrated forest Z-score index[196]. Senf and Seidl used logistic regression to identify four disturbance severity levels based on a set of SC indices calculated using the Land Trendr algorithm[230]. Ground measurements are often needed to convert these SC indices to estimates of disturbance severity measured using physical quantities. For example, field survey data are often used to convert spectral burn indices to ground estimates of burn severity represented using a composite burn index[231-232]. By using field measurements collected by the Forest Inventory and Analysis (FIA) program of the US Forest Service as calibration data, Tao et al. estimated the percentage of basal area removal (PBAR) as a measure of disturbance intensity for disturbance events detected by the VCT algorithm over North Carolina[233]. Building on that study, Lu et al. developed a CONUS-wide disturbance intensity dataset[262].

While fire typically results in an immediate release of most of the carbon stored in aboveground biomass into the atmosphere, timber harvest transfers large portions of the aboveground carbon to the Harvested Wood Product (HWP) pool, which is released to the atmosphere gradually over decades or longer[110, 234]. Carbon fluxes related to the HWP are therefore important components of forest carbon dynamics. The IPCC methods use data provided by the FAO, which provides HWP estimates at the national level for many countries/regions. In the United States, reports on timber product output (TPO) are produced by the FIA program through surveying wood processing mills[235]. These TPO reports make it possible to derive estimates of carbon stored in wood products at county or state levels[110, 236]. Unfortunately, the availability of historical TPO data is highly inconsistent among different states, making it difficult to derive consistent and accurate estimates of carbon stocks and fluxes at regional to national scales[115, 237]. However, the available survey data could be used together with remote sensing-based disturbance data to produce HWP estimates that are spatially and temporally more consistent. For example, available TPO survey data were used to calibrate VCT disturbance products to produce an annual, multi-decadal (1986—2015) TPO record for North Carolina[196], which was then used to estimate the influx of harvested carbon to wood products[238].

4.5 Forthcoming opportunities

Sentinel-1 marks the beginning a new era of no-cost access by the general public to a global archive of systematically-acquired SAR observations. Two new SAR missions with planned launch dates in 2023 likely will also adopt similar no-cost access policies. One is the NASA-ISRO SAR (NISAR) mission being developed by NASA in partnership with ISRO. The other is the BIOMASS mission of the European Space Agency (ESA). NISAR will provide global L-band observations with a 12-day repeat[239]. BIOMASS will deliver crucial information on forest carbon dynamics using P-band observations acquired with a 3-day repeat cycle[240-241]. Along with the existing remote sensing capabilities discussed in section 4.1, these two systems will open new opportunities to advance forest carbon research in several ways.

Given that L-band is more sensitive to high biomass densities than C-band while P-band can penetrate denser canopies than L-band[242], one of the most important improvements provided by the NISAR and BIOMASS missions will be the development of better forest structure and biomass products. Many local studies have demonstrated the value of using multi-band radar data to improve forest monitoring[243-245]. With large quantities of LiDAR samples being collected by GEDI and ICESAT-2 across the globe, integrated use of these samples with observations acquired by Sentinel-1 (C-band), NISAR (L-band), and BIOMASS (P-band) will make it possible to derive more accurate forest structure and biomass products for any region of the globe than currently possible over a wide range of biomass levels.

One of the uncertainty sources in estimating biomass is the lack of information on wood-specific gravity[246], which is often forest type/species dependent. SAR data acquired by the forthcoming NISAR and BIOMASS missions may allow for better mapping of forest species composition. Many studies have demonstrated the usefulness of SAR data for mapping forest type[247-248]. Wolter and Townsend showed that both C-band (Radarsat-1) and L-band (PALSAR) variables were sensitive to the composition and abundance of specific species[249]. Use of SAR imagery with optical data to improve forest type classification has been a focus of many studies[250-252].

Since radar in general is not affected by clouds, the global systematic acquisition capabilities of Sentinel-1, NISAR, and BIOMASS will produce valid observations regardless of solar illumination or atmospheric conditions on a sub-weekly basis across the globe throughout the year. The temporal density of these observations, uncontaminated by cloud or solar illumination conditions, will provide unprecedented temporal details for determining surface phenology. It has been demonstrated that phenology metrics derived using SAR data are comparable to those derived based on optical data[253-254], and SAR observations may provide a unique perspective for characterizing the phenology of tropical[255] and boreal forests[256]. Further, due to rapid vegetation growth following disturbances in many regions, disturbance events are often better detected using observations acquired immediately after those events. Therefore, the high temporal resolutions provided by the forthcoming SAR missions likely will allow for more accurate detection of forest disturbances.

4.6 Need for more and better ground data

Despite the large amount of high-quality LiDAR measurements being collected by GEDI and ICESAT-2, many of the products needed to quantify forest carbon dynamics cannot be derived without ground measurements. For example, although LiDAR metrics are sensitive to tree height and other structural variables[257-259], ground biomass measurements are needed to establish relationships between biomass and LiDAR metrics[260]. Linking ground measurements with space LiDAR samples often requires LiDAR data acquired by airborne systems[146, 261], because the chance for GEDI or other spaceborne LiDAR systems to sample over plot locations where ground measurements already exist is extremely low. In order to account for variations in these relationships, the GEDI team has developed a database of ground-based biomass measurements, which have been used to calibrate relationships between GEDI LiDAR metrics for different regions and plant functional types[178]. However, there are many gaps in the current database. More samples of ground biomass measurements are needed for those gap areas in order to improve the global representativeness of the database.

Similarly, ground samples are needed to establish relationships between disturbance severity and change metrics derived from satellite observations. For the US and other countries that have forest inventory programs that mandate remeasurements over preselected plot locations at specified time intervals, those remeasurements could be used to calculate disturbance severity over plots where disturbances occurred between two measurements[233]. However, because most existing inventory programs are designed to assess the status of forest resources using samples selected following probability-based sampling methods, and forests subject to measurable disturbances within a few years are typically small fractions of all forestland in most regions, the number of plots from two consecutive inventories that could be used to calculate disturbance severity for actual disturbance events is often very small. As a result, those programs may not be able to provide enough samples for quantifying disturbance severity[262]. One way to mitigate this problem is to intensify field sampling over disturbed areas. Given available resources, this could be achieved through well-coordinated field campaigns for cases when the timing and location of certain disturbance events (e.g., planned harvest) are known before the occurrence of those events. Given that the occurrence of natural disturbances is often unpredictable, conducting fieldwork immediately after those disturbances over areas that had pre-disturbance measurements will be highly valuable[263-264].

For forests that are subject to timber harvest, the amount of harvested wood product determines the fate of a significant portion of removed forest biomass carbon. For many countries, however, HWP estimates are only available at the national level. The TPO survey data collected by the FIA program make it possible to develop models for estimating carbon stored in wood products at county or state levels[110, 236]. However, because different countries likely have different timber harvest practices, relationships between HWP and satellite-based disturbance estimates may be different for different countries. Therefore, use of models developed in one state/country to derive sub-national TPO estimates for other countries may not be appropriate. Use of the methods developed by Huang et al.[196] to derive sub-national HWP estimates for other countries will require that those countries collect at least some ground-based HWP data similar to the FIA TPO survey data, which are needed to calibrate and validate the TPO estimation algorithm.

5 Summary

Remote sensing provides an indispensable tool for advancing carbon studies. Data products derived based on remote sensing observations are key inputs to a wide range of models and methods developed for quantifying carbon budget at all levels. Forest carbon inventory methods recommended by the IPCC Guideline require biomass data and a suite of forest disturbance products. Significant progress has been made in deriving these products by leveraging publicly available remote sensing assets, including the long-term imagery record produced by the Landsat mission and observations acquired by several new systems launched within the past decade, including Sentinel-2, Sentinel-1, GEDI, and ICESAT-2. By the time the L-band NISAR and P-band BIOMASS missions are launched in 2023, the Earth's land surface will be imaged by optical and multi-band (including C-, L-, and P-bands) radar systems designed to provide global, sub-weekly observations at sub-hectare spatial resolutions for public use.

Many algorithms have been developed for mapping forest disturbances, determining disturbance attribution, quantifying disturbance intensity, and estimating harvested timber volume. Although the large quantities of globally-distributed LiDAR samples being collected by GEDI and ICESAT-2 can provide much needed reference data critical for calibrating mapping algorithms and validating derived map products, a number of physical quantities needed for calculating forest carbon fluxes cannot be derived from satellite observations without ground-based calibration data. These include biomass, disturbance severity, and harvested wood products. Other important quantities that are more difficult to derive from remote sensing data include dead organic matter and soil carbon. Carefully-designed inventory programs are required in order to collect data needed to estimate these quantities or to provide reference data necessary for calibrating and validating satellite-based estimates.

While the IPCC provides guidelines for carbon inventory at the national scale, carbon trade and other market-driven tools that may help achieve climate mitigation goals through forestry-based carbon management projects require carbon estimates at local or even individual land owner levels. Given that increasingly more fine scale biomass and forest change products will be derived based on existing and forthcoming satellite observations, models that can use these products to produce fine scale carbon fluxes are emerging. In addition to the grid-based carbon accounting models developed by Tang et al.[99-100] and Gong et al.[127], improvements are also being made to other models to enable derivation of fine scale carbon estimates[265]. These evolving modeling capabilities will allow for more robust MRV for REDD+ or other projects aimed at achieving climate mitigation goals through forest management.

Acknowledgement: This study builds on projects funded by NASA's Carbon Cycle Science and Land Cover and Land Use Change Programs, the Laboratory of Environmental Model and Data Optima (EMDO), and PIESAT-Australia. Additional support was provided by the Department of Geographical Sciences of the University of Maryland and the Central Public-Interest Scientific Institution Basic Research Fund (CAFYBB2018GB01). Sophia Huang helped with English editing and proofreading. We thank Professor Jianya Gong for his encouragement and suggestions.

List of Abbreviations/Acronyms

ADS	Aerial Detection Survey
ALOS	Advanced Land Observing Satellite
BEPS	Boreal Ecosystem Productivity Simulator
Biome-BGC	Biome-BioGeochemical Cycles
BLUE	Bookkeeping for Land Use Emission
C2C	Composite2Change
IBIS	Integrated Biosphere Simulator
CASA	Carnegie-Ames-Stanford Approach
CASA GFEDv2	Global Fire Emissions Database, Version 2
CCDC	Continuous Change Detection and Classification
CLM	Community Land Model
CLM-CN	Carbon-Nitrogen
CONUS	Conterminous U.S.
COP	Conference of the Parties
DLEM	Dynamic Land Ecosystem Model
DNDC	DeNitrification and DeComposition

ED	Ecosystem Demography
ER	Ecosystem Respiration
ET	Evapotranspiration
EWMACD	Exponentially Weighted Moving Average Change Detection
FAO	Food and Agriculture Organization
FAPAR	Fraction of Absorbed Photosynthetically Active Radiation
FHM	Forest Health Monitoring program
FIA	Forest Inventory and Analysis program
FIRE-BGC	FIRE BioGeoChemical succession model
FORCLIM	A Climate-sensitive Forest succession ("gap") Model
FOREST-BGC	Forest BioGeoChemical model
FVS	Forest Vegetation Simulator
GEDI	Global Ecosystem Dynamics Investigation
GPP	Gross Primary Production
GtC y^{-1}	Gigaton Carbon per year
HWP	Harvested Wood Products
ICESAT-2	Ice, Cloud and land Elevation Satellite-2
InTEC	Integrated Terrestrial Ecosystem C-budget model
IPCC	Intergovernmental Panel on Climate Change
ISAM	Integrated Science Assessment Model
ISRO	Indian Space Research Organisation
ITRA	Image Trends from Regression Analysis
LANDIS	Landscape Disturbance and Succession model
LandTrendr	Landsat-based Detection of Trends in Disturbance and Recovery
LCMAP	Land Change Monitoring, Assessment, and Projection
LPJ-wsl	Lund-Potsdam-Jena-wald, schnee, landschaft model
LST	Land Surface Temperature
MRV	Monitoring, Reporting, and Verification
MTBS	Monitoring Trends in Burn Severity
NAFD	North American Forest Dynamics
NBP	Net Biome Production
NEE	Net Ecosystem Exchange
NEP	Net Ecosystem Production
NISAR	NASA-ISRO SAR mission
NPP	Net Primary Production
ORCHIDEE	Organising Carbon and Hydrology In Dynamic Ecosystems model
PALSAR	Phased Array L-band Synthetic Aperture Radar
PAR	Photosynthetically Active Radiation
PBAR	Percentage of Basal Area Removal
REDD+	Reducing Emissions from Deforestation and Forest Degradation in Developing Countries
SC	Spectral Change
SiB3	Simple Biosphere Model, Version 3
SIF	Solar-Induced Chlorophyll Fluorescence
TEM	Terrestrial Ecosystem Model

TPO	Timber Product Output
UNFCCC	United Nations Framework Convention on Climate Change
VCT	Vegetation Change Tracker
VIIRS	Visible Infrared Imaging Radiometer Suite
VPD	Vapor-Pressure Deficit
VRDET	Vegetation Regeneration and Disturbance Estimates through Time

References

[1] IPCC. Climate change 2001: The scientific basis[M]. Cambridge: Cambridge University Press, 2001.

[2] IPCC. Climate change 2007: synthesis report. Contribution of working groups Ⅰ, Ⅱ and Ⅲ to the fourth assessment report [M]. Geneva, Switzerland: IPCC, 2007.

[3] CHEN J M. Carbon neutrality: Toward a sustainable future [J]. The Innovation, 2021, 2(3): 100127.

[4] FAHEY T J, WOODBURY P B, BATTLES J J, et al. Forest carbon storage: ecology, management, and policy[J]. Frontiers in Ecology and the Environment, 2010, 8(5): 245-252.

[5] AGRAWAL A, NEPSTAD D, CHHATRE A. Reducing emissions from deforestation and forest degradation[J]. Annual Review of Environment and Resources, 2011, 36: 373-396.

[6] CORBERA E, SCHROEDER H. Governing and implementing REDD+[J]. Environmental Science & Policy, 2011, 14 (2): 89-99.

[7] KÖHL M, NEUPANE P R, MUNDHENK P. REDD+ measurement, reporting and verification—a cost trap? Implications for financing REDD+MRV costs by result-based payments[J]. Ecological Economics, 2020, 168: 106513.

[8] IPCC. 2006 IPCC guidelines for national greenhouse gas inventories. volume 4: agriculture, forestry and other land use[Z]. Japan: IGES, 2006.

[9] IPCC. 2019 Refinement to the 2006 IPCC Guidelines for National Greenhouse Gas Inventories. volume 4: agriculture, forestry and other land use[Z]. Switzerland: IPCC, 2019.

[10] JACKSON R B, BAKER J S. Opportunities and constraints for forest climate mitigation[J]. BioScience, 2010, 60(9): 698-707.

[11] RING I, DRECHSLER M, VAN TEEFFELEN A J, et al. Biodiversity conservation and climate mitigation: what role can economic instruments play? [J]. Current Opinion in Environmental Sustainability, 2010, 2(1-2): 50-58.

[12] GRACE J. Understanding and managing the global carbon cycle [J]. Journal of Ecology, 2004, 92(2): 189-202.

[13] SCHIMEL D S. Terrestrial ecosystems and the carbon cycle[J]. Global Change Biology, 1995, 1(1): 77-91.

[14] SCHIMEL D, PAVLICK R, FISHER J B, et al. Observing terrestrial ecosystems and the carbon cycle from space[J]. Global Change Biology, 2015, 21(5): 1762-1776.

[15] FRIEDLINGSTEIN P, O'SULLIVAN M, JONES M W, et al. Global carbon budget 2020[J]. Earth System Science Data, 2020, 12(4): 3269-3340.

[16] LE QUÉRÉ C, ANDREW R M, FRIEDLINGSTEIN P, et al. Global carbon budget 2017[J]. Earth System Science Data, 2018, 10(1): 405-448.

[17] HOUGHTON R A. Balancing the global carbon budget[J]. Annual Review of Earth and Planetary Sciences, 2007, 35: 313-347.

[18] BONAN G B. Forests and climate change: forcings, feedbacks, and the climate benefits of forests[J]. Science, 2008, 320 (5882): 1444-1449.

[19] HOUGHTON R A. Historic role of forests in the global carbon cycle[M]//KOHLMAIER G H, WEBER M, HOUGHTON R A.Carbon Dioxide Mitigation in Forestry and Wood Industry. Berlin: Springer, 1998: 1-24.

[20] LUYSSAERT S, INGLIMA I, JUNG M, et al. CO_2 balance of boreal, temperate, and tropical forests derived from a global database[J]. Global Change Biology, 2007, 13(12): 2509-2537.

[21] HOUGHTON R A, NASSIKAS A A. Global and regional fluxes of carbon from land use and land cover change 1850—2015 [J]. Global Biogeochemical Cycles, 2017, 31(3): 456-472.

[22] GOWARD S N, MASEK J G, COHEN W, et al. Forest disturbance and North American carbon flux[J]. Eos, Transactions American Geophysical Union, 2008, 89(11): 105-106.

[23] IGBP Terrestrial Carbon Working Group, STEFFEN W, NOBLE I, et al. The terrestrial carbon cycle: implications for the Kyoto protocol[J]. Science, 1998, 280(5368): 1393-1394.

[24] SKOG K E. Sequestration of carbon in harvested wood products for the United States[J]. Forest Products Journal, 2008, 58 (6): 56-72.

[25] ZENG Ning. Carbon sequestration via wood burial[J]. Carbon Balance and Management, 2008, 3(1): 1.

[26] CANADELL J G, RAUPACH M R. Managing forests for climate change mitigation[J]. Science, 2008, 320(5882): 1456-1457.

[27] GOLDEN D, SMITH M A, COLOMBO S. Forest carbon management and carbon trading: a review of Canadian forest options for climate change mitigation [J]. The Forestry Chronicle, 2011, 87(5): 625-635.

[28] SCHULZE E D, VALENTINI R, SANZ M J. The long way from Kyoto to Marrakesh: implications of the Kyoto Protocol negotiations for global ecology[J]. Global Change Biology, 2002, 8(6): 505-518.

[29] BIRDSEY R, PREGITZER K, LUCIER A. Forest carbon management in the United States[J]. Journal of Environmental Quality, 2006, 35(4): 1461-1469.

[30] LAMB R L, HURTT G C, BOUDREAU T J, et al. Context and future directions for integrating forest carbon into subnational climate mitigation planning in the RGGI region of the U.S.[J]. Environmental Research Letters, 2021, 16(6): 063001.

[31] BASTOS A, FRIEDLINGSTEIN P, SITCH S, et al. Impact of the 2015/2016 El Niño on the terrestrial carbon cycle constrained by bottom-up and top-down approaches[J]. Philosophical Transactions of the Royal Society B: Biological Sciences, 2018, 373(1760): 20170304.

[32] SCHIMEL D S, HOUSE J I, HIBBARD K A, et al. Recent patterns and mechanisms of carbon exchange by terrestrial ecosystems[J]. Nature, 2001, 414(6860): 169-172.

[33] HAYES D J, TURNER D P, STINSON G, et al. Reconciling estimates of the contemporary North American carbon balance among terrestrial biosphere models, atmospheric inversions, and a new approach for estimating net ecosystem exchange from inventory-based data[J]. Global Change Biology, 2012, 18(4): 1282-1299.

[34] GURNEY K R, LAW R M, DENNING A S, et al. Towards robust regional estimates of CO_2 sources and sinks using atmospheric transport models[J]. Nature, 2002, 415(6872): 626-630.

[35] STEPHENS B B, GURNEY K R, TANS P P, et al. Weak northern and strong tropical land carbon uptake from vertical profiles of atmospheric CO_2 [J]. Science, 2007, 316(5832): 1732-1735.

[36] FAN S, GLOOR M, MAHLMAN J, et al. A large terrestrial carbon sink in North America implied by atmospheric and oceanic carbon dioxide data and models[J]. Science, 1998, 282(5388): 442-446.

[37] PACALA S W, HURTT G C, BAKER D, et al. Consistent land- and atmosphere-based U.S. carbon sink estimates[J]. Science, 2001, 292(5525): 2316-2320.

[38] GURNEY K R, LAW R M, DENNING A S, et al. TransCom 3 CO_2 inversion intercomparison: 1. annual mean control results and sensitivity to transport and prior flux information[J]. Tellus B: Chemical and Physical Meteorology, 2003, 55(2): 555-579.

[39] HUNTZINGER D N, POST W M, WEI Y, et al. North American Carbon Program (NACP) regional interim synthesis: terrestrial biospheric model intercomparison[J]. Ecological Modelling, 2012, 232: 144-157.

[40] CHEN J M, LIU J, CIHLAR J, et al. Daily canopy photosynthesis model through temporal and spatial scaling for remote sensing applications[J]. Ecological Modelling, 1999, 124(2-3): 99-119.

[41] VAN DER WERF G R, RANDERSON J T, COLLATZ G J, et al. Continental-scale partitioning of fire emissions during the 1997 to 2001 El Nino/La Nina period[J]. Science, 2004, 303(5654): 73-76.

[42] VAN DER WERF G R, RANDERSON J T, GIGLIO L, et al. Interannual variability in global biomass burning emissions from 1997 to 2004[J]. Atmospheric Chemistry and Physics, 2006, 6(11): 3423-3441.

[43] RANDERSON J T, THOMPSON M V, CONWAY T J, et al. The contribution of terrestrial sources and sinks to trends in the seasonal cycle of atmospheric carbon dioxide[J]. Global Biogeochemical Cycles, 1997, 11(4): 535-560.

[44] JAIN A K, YANG Xiaojuan. Modeling the effects of two different land cover change data sets on the carbon stocks of plants and soils in concert with CO_2 and climate change[J]. Global Biogeochemical Cycles, 2005, 19(2): GB2015.

[45] FOLEY J A, PRENTICE I C, RAMANKUTTY N, et al. An integrated biosphere model of land surface processes, terrestrial carbon balance, and vegetation dynamics[J]. Global Biogeochemical Cycles, 1996, 10(4): 603-628.

[46] THORNTON P E, DONEY S C, LINDSAY K, et al. Carbon-nitrogen interactions regulate climate-carbon cycle feedbacks: results from an atmosphere-ocean general circulation model [J]. Biogeosciences, 2009, 6(10): 2099-2120.

[47] TIAN Hanqin, CHEN Guangsheng, LIU Mingliang, et al. Model estimates of net primary productivity, evapotranspiration, and water use efficiency in the terrestrial ecosystems of the southern United States during 1895—2007[J]. Forest Ecology and Management, 2010, 259(7): 1311-1327.

[48] SITCH S, SMITH B, PRENTICE I C, et al. Evaluation of ecosystem dynamics, plant geography and terrestrial carbon cycling in the LPJ dynamic global vegetation model[J]. Global Change Biology, 2003, 9(2): 161-185.

[49] KRINNER G, VIOVY N, DE NOBLET-DUCOUDRÉN, et al. A dynamic global vegetation model for studies of the coupled atmosphere-biosphere system[J]. Global Biogeochemical Cycles, 2005, 19(1): GB1015.

[50] BAKER I T, PRIHODKO L, DENNING A S, et al. Seasonal drought stress in the Amazon: reconciling models and observations[J]. Journal of Geophysical Research: Biogeosciences, 2008, 113(G1): G00B01.

[51] RAICH J W, RASTETTER E B, MELILLO J M, et al. Potential net primary productivity in South America: application of a global model[J]. Ecological Applications, 1991, 1(4): 399-429.

[52] LIU Shuguang, BOND-LAMBERTY B, HICKE J A, et al. Simulating the impacts of disturbances on forest carbon cycling in North America: processes, data, models, and challenges[J]. Journal of Geophysical Research: Biogeosciences, 2011, 116(G4): G00K08.

[53] JU Weimin, CHEN J M, BLACK T A, et al. Modelling multi-year coupled carbon and water fluxes in a boreal aspen forest [J]. Agricultural and Forest Meteorology, 2006, 140(1-4): 136-151.

[54] BOND-LAMBERTY B, GOWER S T, AHL D E, et al. Re-

implementation of the Biome-BGC model to simulate successional change[J]. Tree Physiology, 2005, 25(4): 413-424.
[55] KUCHARIK C J, FOLEY J A, DELIRE C, et al. Testing the performance of a dynamic global ecosystem model: water balance, carbon balance, and vegetation structure[J]. Global Biogeochemical Cycles, 2000, 14(3): 795-825.
[56] PARTON W J, OJIMA D S, COLE C V, et al. A general model for soil organic matter dynamics: sensitivity to litter chemistry, texture and management[M] // BRYANT R B, ARNOLD R W. Quantitative Modeling of Soil Forming Processes. Soil Science Society of America, 1994, 39: 147-167.
[57] RANDERSON J T, HOFFMAN F M, THORNTON P E, et al. Systematic assessment of terrestrial biogeochemistry in coupled climate-carbon models[J]. Global Change Biology, 2009, 15(10): 2462-2484.
[58] LI Changsheng, FROLKING S, CROCKER G J, et al. Simulating trends in soil organic carbon in long-term experiments using the DNDC model[J]. Geoderma, 1997, 81(1-2): 45-60.
[59] HURTT G C, MOORCROFT P R, AND S W P, et al. Terrestrial models and global change: challenges for the future[J]. Global Change Biology, 1998, 4(5): 581-590.
[60] MOORCROFT P R, HURTT G C, PACALA S W. A method for scaling vegetation dynamics: the ecosystem demography model[J]. Ecological Monographs, 2001, 71(4): 557-586.
[61] LIU Shuguang, BLISS N, SUNDQUIST E, et al. Modeling carbon dynamics in vegetation and soil under the impact of soil erosion and deposition[J]. Global Biogeochemical Cycles, 2003, 17(2): 1074.
[62] KEANE R E, RYAN K C, RUNNING S W. Simulating effects of fire on northern Rocky Mountain landscapes with the ecological process model FIRE-BGC[J]. Tree Physiology, 1996, 16(3): 319-331.
[63] BUGMANN H. On the ecology of mountainous forests in a changing climate: a simulation study[D]. Zurich: ETH Zurich, 1994.
[64] RUNNING S W, GOWER S T. FOREST-BGC, A general model of forest ecosystem processes for regional applications. II. Dynamic carbon allocation and nitrogen budgets[J]. Tree Physiology, 1991, 9(1-2): 147-160.
[65] DIXON G E. Essential FVS: A user's guide to the forest vegetation simulator[R]. Fort Collins, CO: US Department of Agriculture, Forest Service, Forest Management Service Center, 2002.
[66] FRIEND A D, STEVENS A K, KNOX R G, et al. A process-based, terrestrial biosphere model of ecosystem dynamics (Hybrid v3.0)[J]. Ecological Modelling, 1997, 95(2-3): 249-287.
[67] CHEN Wenjun, CHEN Jing, CIHLAR J. An integrated terrestrial ecosystem carbon-budget model based on changes in disturbance, climate, and atmospheric chemistry[J]. Ecological Modelling, 2000, 135(1): 55-79.
[68] MLADENOFF D J. LANDIS and forest landscape models[J]. Ecological Modelling, 2004, 180(1): 7-19.
[69] PASTOR J, POST W M. Influence of climate, soil moisture, and succession on forest carbon and nitrogen cycles[J]. Biogeochemistry, 1986, 2(1): 3-27.
[70] BONDEAU A, SMITH P C, ZAEHLE S, et al. Modelling the role of agriculture for the 20th century global terrestrial carbon balance[J]. Global Change Biology, 2007, 13(3): 679-706.
[71] PACALA S W, CANHAM C D, SAPONARA J, et al. Forest models defined by field measurements: estimation, error analysis and dynamics[J]. Ecological Monographs, 1996, 66(1): 1-43.
[72] MCGUIRE A D, MELILLO J M, JOYCE L A, et al. Interactions between carbon and nitrogen dynamics in estimating net primary productivity for potential vegetation in North America[J]. Global Biogeochemical Cycles, 1992, 6(2): 101-124.
[73] PAN Y, CHEN J M, BIRDSEY R, et al. Age structure and disturbance legacy of North American forests[J]. Biogeosciences Discussions, 2010, 7(1): 979-1020.
[74] NORBY R J, OGLE K, CURTIS P S, et al. Aboveground growth and competition in forest gap models: an analysis for studies of climatic change[J]. Climatic Change, 2001, 51(3): 415-447.
[75] LAW B E, TURNER D, CAMPBELL J, et al. Disturbance and climate effects on carbon stocks and fluxes across Western Oregon USA[J]. Global Change Biology, 2004, 10(9): 1429-1444.
[76] WANG Weile, ICHII K, HASHIMOTO H, et al. A hierarchical analysis of terrestrial ecosystem model Biome-BGC: equilibrium analysis and model calibration[J]. Ecological Modelling, 2009, 220(17): 2009-2023.
[77] BUGMANN H. A review of forest gap models[J]. Climatic Change, 2001, 51(3-4): 259-305.
[78] WULLSCHLEGER S D, JACKSON R B, CURRIE W S, et al. Below-ground processes in gap models for simulating forest response to global change[J]. Climatic Change, 2001, 51(3-4): 449-473.
[79] HURTT G C, PACALA S W, MOORCROFT P R, et al. Projecting the future of the U.S. carbon sink[J]. Proceedings of the National Academy of Sciences of the United States of America, 2002, 99(3): 1389-1394.
[80] CROOKSTON N L, REHFELDT G E, DIXON G E, et al. Addressing climate change in the forest vegetation simulator to assess impacts on landscape forest dynamics[J]. Forest Ecology and Management, 2010, 260(7): 1198-1211.
[81] HOUGHTON R A. Land-use change and the carbon cycle[J]. Global Change Biology, 1995, 1(4): 275-287.
[82] HOUGHTON R A. How well do we know the flux of CO_2 from land-use change? [J]. Tellus B: Chemical and Physical Meteorology, 2010, 62(5): 337-351.
[83] HOUGHTON R A, HOBBIE J E, MELILLO J M, et al. Changes in the carbon content of terrestrial biota and soils be-

tween 1860 and 1980: A net release of CO_2 to the atmosphere [J]. Ecological Monographs, 1983, 53(3): 235-262.

[84] HOUGHTON R A. The annual net flux of carbon to the atmosphere from changes in land use 1850—1990[J]. Tellus B: Chemical and Physical Meteorology, 1999, 51(2): 298-313.

[85] HOUGHTON R A. Revised estimates of the annual net flux of carbon to the atmosphere from changes in land use and land management 1850—2000 [J]. Tellus B: Chemical and Physical Meteorology, 2003, 55(2): 378-390.

[86] HOUGHTON R A, HACKLER J L, LAWRENCE K T. The U.S. carbon budget: contributions from land-use change[J]. Science, 1999, 285(5427): 574-578.

[87] HOUGHTON R A, HACKLER J L. Sources and sinks of carbon from land-use change in China [J]. Global Biogeochemical Cycles, 2003, 17(2): 1034.

[88] HOUGHTON R A, SKOLE D L, NOBRE C A, et al. Annual fluxes of carbon from deforestation and regrowth in the Brazilian Amazon[J]. Nature, 2000, 403(6767): 301-304.

[89] HARRIS N L, BROWN S, HAGEN S C, et al. Baseline map of carbon emissions from deforestation in tropical regions[J]. Science, 2012, 336(6088): 1573-1576.

[90] ANDERSEN L E, DOYLE A S, GRANADO S D, et al. Net carbon emissions from deforestation in Bolivia during 1990—2000 and 2000—2010: Results from a Carbon Bookkeeping Model[J]. PLoS One, 2016, 11(3): e0151241.

[91] BACCINI A, GOETZ S J, WALKER W S, et al. Estimated carbon dioxide emissions from tropical deforestation improved by carbon-density maps[J]. Nature Climate Change, 2012, 2(3): 182-185.

[92] ACHARD F, EVA H D, MAYAUX P, et al. Improved estimates of net carbon emissions from land cover change in the tropics for the 1990s [J]. Global Biogeochemical Cycles, 2004, 18(2): GB2008.

[93] HANSIS E, DAVIS S J, PONGRATZ J. Relevance of methodological choices for accounting of land use change carbon fluxes[J]. Global Biogeochemical Cycles, 2015, 29(8): 1230-1246.

[94] GASSER T, CIAIS P. A theoretical framework for the net land-to-atmosphere CO_2 flux and its implications in the definition of "emissions from land-use change"[J]. Earth System Dynamics, 2013, 4(1): 171-186.

[95] REICK C, RADDATZ T, PONGRATZ J, et al. Contribution of anthropogenic land cover change emissions to pre-industrial atmospheric CO_2[J]. Tellus B: Chemical and Physical Meteorology, 2010, 62(5): 329-336.

[96] SHEVLIAKOVA E, STOUFFER R J, MALYSHEV S, et al. Historical warming reduced due to enhanced land carbon uptake [C] // Proceedings of the National Academy of Sciences of the United States of America, 2013, 110(42): 16730-16735.

[97] STOCKER B D, FEISSLI F, STRASSMANN K M, et al. Past and future carbon fluxes from land use change, shifting cultivation and wood harvest[J]. Tellus B: Chemical and Physical Meteorology, 2014, 66(1): 23188.

[98] WILKENSKJELD S, KLOSTER S, PONGRATZ J, et al. Comparing the influence of net and gross anthropogenic land-use and land-cover changes on the carbon cycle in the MPI-ESM[J]. Biogeosciences, 2014, 11(17): 4817-4828.

[99] TANG Xiaojing, HUTYRA L R, ARÉVALO P, et al. Spatiotemporal tracking of carbon emissions and uptake using time series analysis of Landsat data: a spatially explicit carbon bookkeeping model[J]. Science of the Total Environment, 2020, 720: 137409.

[100] TANG Xiaojing, WOODCOCK C E, OLOFSSON P, et al. Spatiotemporal assessment of land use/land cover change and associated carbon emissions and uptake in the Mekong River Basin [J]. Remote Sensing of Environment, 2021, 256: 112336.

[101] GILLIS M D, OMULE A Y, BRIERLEY T. Monitoring Canada's forests: the national forest inventory[J]. The Forestry Chronicle, 2005, 81(2): 214-221.

[102] NELSON M, MOISEN G, FINCO M, et al. Forest inventory and analysis in the United States: remote sensing and geospatial activities [J]. Photogrammetric Engineering and Remote Sensing, 2007, 73(7): 729-732.

[103] SMITH W B. Forest inventory and analysis: a national inventory and monitoring program[J]. Environmental Pollution, 2002, 116(S1): S233-S242.

[104] JENKINS J C, BIRDSEY R A, PAN Yude. Biomass and NPP estimation for the mid-Atlantic region (USA) using plot-level forest inventory data [J]. Ecological Applications, 2001, 11(4): 1174-1193.

[105] JENKINS J C, CHOJNACKY D C, HEATH L S, et al. National scale biomass estimators for United States tree species [J]. Forest Science, 2003, 49(1): 12-35.

[106] BIRDSEY R A. Carbon storage and accumulation in United States forest ecosystems[R]. Washington, DC: U.S. Department of Agriculture, Forest Service, 1992.

[107] BIRDSEY R A, HEATH L S. Carbon changes in U.S. forests [M]//JOYCE L A. Productivity of America's Forests and Climate Change. Fort Collins, Colorado: USDA, Forest Service: 1995: 56-70.

[108] TURNER D P, KOERPER G J, HARMON M E, et al. A carbon budget for forests of the conterminous United States [J]. Ecological Applications, 1995, 5(2): 421-436.

[109] HEATH L S, SMITH J E, SKOG K E, et al. Managed forest carbon estimates for the US greenhouse gas inventory, 1990-2008[J]. Journal of Forestry, 2011, 109(3): 167-173.

[110] SMITH J E, HEATH L S, SKOG K E, et al. Methods for calculating forest ecosystem and harvested carbon with standard estimates for forest types of the United States[R]. Newtown Square, PA: USDA, Forest Service, 2006.

[111] STINSON G, KURZ W A, SMYTH C E, et al. An inventory-based analysis of Canada's managed forest carbon dynamics,

1990 to 2008[J]. Global Change Biology, 2011, 17(6): 2227-2244.

[112] SHVIDENKO A, NILSSON S. Dynamics of Russian forests and the carbon budget in 1961—1998: An assessment based on long-term forest inventory data[J]. Climatic Change, 2002, 55(1-2): 5-37.

[113] JANSSENS I A, FREIBAUER A, CIAIS P, et al. Europe's terrestrial biosphere absorbs 7% to 12% of European anthropogenic CO_2 emissions[J]. Science, 2003, 300(5625): 1538-1542.

[114] NABUURS G J, SCHELHAAS M J, MOHREN G F M J, et al. Temporal evolution of the European forest sector carbon sink from 1950 to 1999[J]. Global Change Biology, 2003, 9(2): 152-160.

[115] BIRDSEY R. Data gaps for monitoring forest carbon in the United States: an inventory perspective[J]. Environmental Management, 2004, 33(1): S1-S8.

[116] ŤUPEK B, ZANCHI G, VERKERK P J, et al. A comparison of alternative modelling approaches to evaluate the European forest carbon fluxes[J]. Forest Ecology and Management, 2010, 260(3): 241-251.

[117] WOODALL C W, COULSTON J W, DOMKE G M, et al. The U.S. forest carbon accounting framework: stocks and stock change, 1990—2016[R]. Newtown Square, PA: U.S. Department of Agriculture, Forest Service, Northern Research Station, 2015.

[118] KURZ W A, DYMOND C C, WHITE T M, et al. CBM-CFS3: A model of carbon-dynamics in forestry and land-use change implementing IPCC standards[J]. Ecological Modelling, 2009, 220(4): 480-504.

[119] RICHARDS G P, EVANS D M W. Development of a carbon accounting model (FullCAM Vers. 1.0) for the Australian continent[J]. Australian Forestry, 2004, 67(4): 277-283.

[120] PETRESCU A M R, PETERS G P, JANSSENS-MAENHOUT G, et al. European anthropogenic AFOLU greenhouse gas emissions: a review and benchmark data[J]. Earth System Science Data, 2020, 12(2): 961-1001.

[121] UMEMIYA C, WHITE M, AMELLINA A, et al. National greenhouse gas inventory capacity: an assessment of Asian developing countries[J]. Environmental Science & Policy, 2017, 78: 66-73.

[122] XIAO Jingfeng, CHEVALLIER F, GOMEZ C, et al. Remote sensing of the terrestrial carbon cycle: a review of advances over 50 years[J]. Remote Sensing of Environment, 2019, 233: 111383.

[123] HILKER T, COOPS N C, WULDER M A, et al. The use of remote sensing in light use efficiency based models of gross primary production: a review of current status and future requirements[J]. Science of the Total Environment, 2008, 404(2-3): 411-423.

[124] LADONI M, BAHRAMI H A, ALAVIPANAH S K, et al. Estimating soil organic carbon from soil reflectance: a review[J]. Precision Agriculture, 2010, 11(1): 82-99.

[125] GOETZ S, DUBAYAH R. Advances in remote sensing technology and implications for measuring and monitoring forest carbon stocks and change[J]. Carbon Management, 2011, 2(3): 231-244.

[126] RYU Y, BERRY J A, BALDOCCHI D D. What is global photosynthesis? History, uncertainties and opportunities[J]. Remote Sensing of Environment, 2019, 223: 95-114.

[127] GONG Weishu, HUANG Chengquan, HOUGHTON R A, et al. Carbon fluxes from contemporary forest disturbances in North Carolina evaluated using a grid-based carbon accounting model and fine resolution remote sensing products[J]. Science of Remote Sensing, 2022, 5: 100042.

[128] WULDER M A, LOVELAND T R, ROY D P, et al. Current status of Landsat program, science, and applications[J]. Remote Sensing of Environment, 2019, 225: 127-147.

[129] LOVELAND T R, DWYER J L. Landsat: bilding a strong future[J]. Remote Sensing of Environment, 2012, 122: 22-29.

[130] DABBOOR M, OLTHOF I, MAHDIANPARI M, et al. The RADARSAT constellation mission core applications: first results[J]. Remote Sensing, 2022, 14(2): 301.

[131] ROSENQVIST A, SHIMADA M, SUZUKI S, et al. Operational performance of the ALOS global systematic acquisition strategy and observation plans for ALOS-2 PALSAR-2[J]. Remote Sensing of Environment, 2014, 155: 3-12.

[132] WOODCOCK C E, ALLEN R, ANDERSON M, et al. Free access to landsat imagery[J]. Science, 2008, 320(5879): 1011.

[133] DRUSCH M, DEL BELLO U, CARLIER S, et al. Sentinel-2: ESA's optical high-resolution mission for GMES operational services[J]. Remote Sensing of Environment, 2012, 120: 25-36.

[134] POTIN P, ROSICH B, MIRANDA N, et al. Sentinel-1 mission status[J]. Procedia Computer Science, 2016, 100: 1297-1304.

[135] NEUENSCHWANDER A, PITTS K. The ATL08 land and vegetation product for the ICESat-2 Mission[J]. Remote Sensing of Environment, 2019, 221: 247-259.

[136] DUBAYAH R, BLAIR J B, GOETZ S, et al. The global ecosystem dynamics investigation: high-resolution laser ranging of the Earth's forests and topography[J]. Science of Remote Sensing, 2020, 1: 100002.

[137] HOUGHTON R A. Aboveground forest biomass and the global carbon balance[J]. Global Change Biology, 2005, 11(6): 945-958.

[138] HOUGHTON R A, HALL F, GOETZ S J. Importance of biomass in the global carbon cycle[J]. Journal of Geophysical Research: Biogeosciences, 2009, 114(G2): G00E03.

[139] DUBAYAH R O, DRAKE J B. Lidar remote sensing for forestry[J]. Journal of Forestry, 2000, 98(6): 44-46.

[140] LEFSKY M A, COHEN W B, ACKER S A, et al. Lidar re-

mote sensing of the canopy structure and biophysical properties of douglas-fir western hemlock forests[J]. Remote Sensing of Environment, 1999, 70(3): 339-361.

[141] LEFSKY M A, COHEN W B, HARDING D J, et al. Lidar remote sensing of above-ground biomass in three biomes[J]. Global Ecology and Biogeography, 2002, 11(5): 393-399.

[142] NELSON R, MARGOLIS H, MONTESANO P, et al. Lidar-based estimates of aboveground biomass in the continental US and Mexico using ground, airborne, and satellite observations[J]. Remote Sensing of Environment, 2017, 188: 127-140.

[143] PANG Yong, WANG Weiwei, DU Liming, et al. Nyström-based spectral clustering using airborne LiDAR point cloud data for individual tree segmentation[J]. International Journal of Digital Earth, 2021, 14(10): 1452-1476.

[144] WANG Qiang, PANG Yong, CHEN Dongsheng, et al. Lidar biomass index: a novel solution for tree-level biomass estimation using 3D crown information[J]. Forest Ecology and Management, 2021, 499: 119542.

[145] PANG Yong, LI Zengyuan. Inversion of biomass components of the temperate forest using airborne Lidar technology in Xiaoxing'an Mountains, Northeastern of China[J]. Chinese Journal of Plant Ecology, 2012, 36(10): 1095-1105.

[146] PANG Yong, LI Zengyuan, MENG Shili, et al. China typical forest aboveground biomass estimation by fusion of multi-platform data[C]// Proceedings of the 2016 IEEE International Geoscience and Remote Sensing Symposium (IGARSS). Beijing: IEEE, 2016: 3557-3560.

[147] PANG Yong, LI Zengyuan. Subtropical forest biomass estimation using airborne LiDAR and Hyperspectral data[J]. The International Archives of the Photogrammetry, Remote Sensing and Spatial Information Sciences, 2016, XLI-B8: 747-749.

[148] RIGNOT E, WAY J B, MCDONALD K, et al. Monitoring of environmental conditions in Taiga forests using ERS-1 SAR [J]. Remote Sensing of Environment, 1994, 49(2): 145-154.

[149] NEEFF T, DE ALENCASTRO GRAÇA P M, DUTRA L V, et al. Carbon budget estimation in Central Amazonia: Successional forest modeling from remote sensing data[J]. Remote Sensing of Environment, 2005, 94(4): 508-522.

[150] RAUSTE Y. Multi-temporal JERS SAR data in boreal forest biomass mapping[J]. Remote Sensing of Environment, 2005, 97(2): 263-275.

[151] PULLIAINEN J, ENGDAHL M, HALLIKAINEN M. Feasibility of multi-temporal interferometric SAR data for stand-level estimation of boreal forest stem volume[J]. Remote Sensing of Environment, 2003, 85(4): 397-409.

[152] PATENAUDE G, MILNE R, DAWSON T P. Synthesis of remote sensing approaches for forest carbon estimation: reporting to the Kyoto Protocol[J]. Environmental Science & Policy, 2005, 8(2): 161-178.

[153] AUSTIN J M, MACKEY B G, VAN NIEL K P. Estimating forest biomass using satellite radar: an exploratory study in a temperate Australian Eucalyptus forest[J]. Forest Ecology and Management, 2003, 176(1-3): 575-583.

[154] BALZTER H, SKINNER L, LUCKMAN A, et al. Estimation of tree growth in a conifer plantation over 19 years from multi-satellite L-band SAR[J]. Remote Sensing of Environment, 2003, 84(2): 184-191.

[155] SANTOS J R, FREITAS C C, ARAUJO L S, et al. Airborne P-band SAR applied to the aboveground biomass studies in the Brazilian tropical rainforest[J]. Remote Sensing of Environment, 2003, 87(4): 482-493.

[156] RAUSTE Y. Multi-temporal JERS SAR data in boreal forest biomass mapping[J]. Remote Sensing of Environment, 2005, 97(2): 263-275.

[157] FRANSSON J E S, WALTER F, ULANDER L M H. Estimation of forest parameters using CARABAS-II VHF SAR data[J]. IEEE Transactions on Geoscience and Remote Sensing, 2000, 38(2): 720-727.

[158] SANTOS J R, FREITAS C C, ARAUJO L S, et al. Airborne P-band SAR applied to the aboveground biomass studies in the Brazilian tropical rainforest[J]. Remote Sensing of Environment, 2003, 87(4): 482-493.

[159] SCHRÖDER R, PULS J, HAJNSEK I, et al. MAPSAR: a small L-band SAR mission for land observation[J]. Acta Astronautica, 2005, 56(1-2): 35-43.

[160] BALZTER H, SKINNER L, LUCKMAN A, et al. Estimation of tree growth in a conifer plantation over 19 years from multi-satellite L-band SAR[J]. Remote Sensing of Environment, 2003, 84(2): 184-191.

[161] CASTEL T, GUERRA F, CARAGLIO Y, et al. Retrieval biomass of a large Venezuelan pine plantation using JERS-1 SAR data. Analysis of forest structure impact on radar signature[J]. Remote Sensing of Environment, 2002, 79(1): 30-41.

[162] DONOGHUE D N M, WATT P J. Using LiDAR to compare forest height estimates from IKONOS and Landsat ETM+ data in Sitka spruce plantation forests[J]. International Journal of Remote Sensing, 2006, 27(11): 2161-2175.

[163] HYYPPÄ J, HYYPPÄ H, INKINEN M, et al. Accuracy comparison of various remote sensing data sources in the retrieval of forest stand attributes[J]. Forest Ecology and Management, 2000, 128(1-2): 109-120.

[164] MENG Shili, PANG Yong, ZHANG Zhongjun, et al. Mapping aboveground biomass using texture indices from aerial photos in a temperate forest of northeastern China[J]. Remote Sensing, 2016, 8(3): 230.

[165] POWELL S L, COHEN W B, HEALEY S P, et al. Quantification of live aboveground forest biomass dynamics with Landsat time-series and field inventory data: a comparison of empirical modeling approaches[J]. Remote Sensing of Environment, 2010, 114(5): 1053-1068.

[166] JI Lei, WYLIE B K, NOSSOV D R, et al. Estimating aboveground biomass in interior Alaska with Landsat data and field measurements[J]. International Journal of Applied Earth Observation and Geoinformation, 2012, 18: 451-461.

[167] MATASCI G, HERMOSILLA T, WULDER M A, et al. Large-area mapping of Canadian boreal forest cover, height, biomass and other structural attributes using Landsat composites and lidar plots[J]. Remote Sensing of Environment, 2018, 209: 90-106.

[168] KELLNDORFER J, WALKER W, KIRSCH K, et al. NACP aboveground biomass and carbon baseline data, V. 2 (NBCD 2000), U.S.A., 2000[R]. Oak Ridge, Tennessee: ORNL Distributed Active Archive Center, 2013.

[169] BLACKARD J A, FINCO M V, HELMER E H, et al. Mapping U.S. forest biomass using nationwide forest inventory data and moderate resolution information [J]. Remote Sensing of Environment, 2008, 112(4): 1658-1677.

[170] WILSON B T, WOODALL C W, GRIFFITH D M. Imputing forest carbon stock estimates from inventory plots to a nationally continuous coverage[J]. Carbon Balance and Management, 2013, 8(1): 1.

[171] ZHANG Xiaoyang, KONDRAGUNTA S. Estimating forest biomass in the USA using generalized allometric models and MODIS land products[J]. Geophysical Research Letters, 2006, 33(9): L09402.

[172] CHI Hong, SUN Guoqing, HUANG Jinliang, et al. National forest aboveground biomass mapping from ICESat/GLAS data and MODIS imagery in China[J]. Remote Sensing, 2015, 7(5): 5534-5564.

[173] SU Yanjun, GUO Qinghua, XUE Baolin, et al. Spatial distribution of forest aboveground biomass in China: estimation through combination of spaceborne lidar, optical imagery, and forest inventory data [J]. Remote Sensing of Environment, 2016, 173: 187-199.

[174] BACCINI A, LAPORTE N, GOETZ S J, et al. A first map of tropical Africa's above-ground biomass derived from satellite imagery[J]. Environmental Research Letters, 2008, 3(4): 045011.

[175] SAATCHI S S, HARRIS N L, BROWN S, et al. Benchmark map of forest carbon stocks in tropical regions across three continents[J]. Proceedings of the National Academy of Sciences of the United States of America, 2011, 108(24): 9899-9904.

[176] HUANG Huabing, LIU Caixia, WANG Xiaoyi, et al. Integration of multi-resource remotely sensed data and allometric models for forest aboveground biomass estimation in China [J]. Remote Sensing of Environment, 2019, 221: 225-234.

[177] HEALEY S P, YANG Zhiqiang, GORELICK N, et al. Highly local model calibration with a new GEDI LiDAR asset on google earth engine reduces landsat forest height signal saturation[J]. Remote Sensing, 2020, 12(17): 2840.

[178] DUNCANSON L, KELLNER J R, ARMSTON J, et al. Aboveground biomass density models for NASA's Global Ecosystem Dynamics Investigation (GEDI) lidar mission [J]. Remote Sensing of Environment, 2022, 270: 112845.

[179] SAARELA S, HOLM S, HEALEY S P, et al. Generalized hierarchical model-based estimation for aboveground biomass assessment using GEDI and landsat data [J]. Remote Sensing, 2018, 10(11): 1832.

[180] DUNCANSON L, NEUENSCHWANDER A, HANCOCK S, et al. Biomass estimation from simulated GEDI, ICESat-2 and NISAR across environmental gradients in Sonoma County, California [J]. Remote Sensing of Environment, 2020, 242: 111779.

[181] SILVA C A, DUNCANSON L, HANCOCK S, et al. Fusing simulated GEDI, ICESat-2 and NISAR data for regional aboveground biomass mapping[J]. Remote Sensing of Environment, 2021, 253: 112234.

[182] ALBINET C, WHITEHURST A S, JEWELL L A, et al. A joint ESA-NASA Multi-mission Algorithm and Analysis Platform (MAAP) for biomass, NISAR, and GEDI[J]. Surveys in Geophysics, 2019, 40(4): 1017-1027.

[183] LI A, et al. Mapping forest height for Mississippi using long-term landsat observations and GLAS data[EB/OL].[2022-04-12] https://cce.nasa.gov/meeting_te_2010/abs_and_discussions/te2010_ab_searchab_id108.html

[184] NEIGH C S R, MASEK J G, BOURGET P, et al. Deciphering the precision of stereo IKONOS canopy height models for US forests with G-LiHT airborne LiDAR [J]. Remote Sensing, 2014, 6(3): 1762-1782.

[185] POTAPOV P, LI Xinyuan, HERNANDEZ-SERNA A, et al. Mapping global forest canopy height through integration of GEDI and Landsat data[J]. Remote Sensing of Environment, 2021, 253: 112165.

[186] RISHMAWI K, HUANG Chengquan, ZHAN Xiwu. Monitoring key forest structure attributes across the conterminous united states by integrating GEDI LiDAR measurements and VIIRS data[J]. Remote Sensing, 2021, 13(3): 442.

[187] FELDPAUSCH T R, LLOYD J, LEWIS S L, et al. Tree height integrated into pantropical forest biomass estimates [J]. Biogeosciences, 2012, 9(8): 3381-3403.

[188] LI Haikui, ZHAO Pengxiang. Improving the accuracy of tree-level aboveground biomass equations with height classification at a large regional scale[J]. Forest Ecology and Management, 2013, 289: 153-163.

[189] HUANG Chengquan, GOWARD S N, MASEK J G, et al. Development of time series stacks of Landsat images for reconstructing forest disturbance history[J]. International Journal of Digital Earth, 2009, 2(3): 195-218.

[190] HUANG Chengquan, GOWARD S N, MASEK J G, et al. An automated approach for reconstructing recent forest disturbance history using dense Landsat time series stacks[J]. Remote Sensing of Environment, 2010, 114(1): 183-198.

[191] HUANG Chengquan, GOWARD S N, SCHLEEWEIS K, et al.

Dynamics of national forests assessed using the Landsat record: case studies in eastern United States[J]. Remote Sensing of Environment, 2009, 113(7): 1430-1442.

[192] THOMAS N E, HUANG Chengquan, GOWARD S N, et al. Validation of North American Forest Disturbance dynamics derived from Landsat time series stacks[J]. Remote Sensing of Environment, 2011, 115(1): 19-32.

[193] GOWARD S N, HUANG C, ZHAO F, et al. NACP NAFD project: forest disturbance history from Landsat, 1986-2010 [Z]. Oak Ridge, Tennessee: ORNL DAAC, 2016.

[194] ZHAO Feng, HUANG Chengquan, GOWARD S N, et al. Development of Landsat-based annual US forest disturbance history maps (1986—2010) in support of the North American Carbon Program (NACP)[J]. Remote Sensing of Environment, 2018, 209: 312-326.

[195] HEALEY S P, COHEN W B, YANG Zhiqiang, et al. Mapping forest change using stacked generalization: an ensemble approach[J]. Remote Sensing of Environment, 2018, 204: 717-728.

[196] HUANG Chengquan, LING P Y, ZHU Zhiliang. North Carolina's forest disturbance and timber production assessed using time series Landsat observations[J]. International Journal of Digital Earth, 2015, 8(12): 947-969.

[197] HUANG C, SCHLEEWEIS K, THOMAS N, et al. Forest dynamics within and around the Olympic National Park assessed using time series Landsat observations[M]// WANG Y. Remote Sensing of Protected Lands. London: Taylor & Francis, 2011: 71-93.

[198] EIDENSHINK J, SCHWIND B, BREWER K, et al. A project for monitoring trends in burn severity[J]. Fire Ecology, 2007, 3(1): 3-21.

[199] WILLIAMS D W, BIRDSEY R A. Historical patterns of spruce budworm defoliation and bark beetle outbreaks in North American conifer forests: an atlas and description of digital maps[R]. Newtown Square, PA: USDS, Forest Service, Northeastern Research Station, 2003.

[200] MEDDENS A J H, HICKE J A, FERGUSON C A. Spatiotemporal patterns of observed bark beetle-caused tree mortality in British Columbia and the western United States [J]. Ecological Applications, 2012, 22(7): 1876-1891.

[201] ZENG Hongcheng, CHAMBERS J Q, NEGRÓN-JUÁREZ R I, et al. Impacts of tropical cyclones on U. S. forest tree mortality and carbon flux from 1851 to 2000[J]. Proceedings of the National Academy of Sciences of the United States of America, 2009, 106(19): 7888-7892.

[202] KENNEDY R E, COHEN W B, SCHROEDER T A. Trajectory-based change detection for automated characterization of forest disturbance dynamics[J]. Remote Sensing of Environment, 2007, 110(3): 370-386.

[203] KENNEDY R E, YANG Zhiqiang, COHEN W B. Detecting trends in forest disturbance and recovery using yearly Landsat time series: 1. Land Trendr-Temporal segmentation algorithms [J]. Remote Sensing of Environment, 2010, 114(12): 2897-2910.

[204] ZHU Zhe, WOODCOCK C E. Continuous change detection and classification of land cover using all available Landsat data[J]. Remote Sensing of Environment, 2014, 144: 152-171.

[205] HERMOSILLA T, WULDER M A, WHITE J C, et al. An integrated Landsat time series protocol for change detection and generation of annual gap-free surface reflectance composites[J]. Remote Sensing of Environment, 2015, 158: 220-234.

[206] HERMOSILLA T, WULDER M A, WHITE J C, et al. Mass data processing of time series Landsat imagery: pixels to data products for forest monitoring[J]. International Journal of Digital Earth, 2016, 9(11): 1035-1054.

[207] BROOKS E B, WYNNE R H, THOMAS V A, et al. On-the-fly massively multitemporal change detection using statistical quality control charts and landsat data[J]. IEEE Transactions on Geoscience and Remote Sensing, 2014, 52(6): 3316-3332.

[208] HUGHES M J, KAYLOR S D, HAYES D J. Patch-based forest change detection from landsat time series[J]. Forests, 2017, 8(5): 166.

[209] VOGELMANN J E, XIAN G, HOMER C, et al. Monitoring gradual ecosystem change using Landsat time series analyses: case studies in selected forest and rangeland ecosystems[J]. Remote Sensing of Environment, 2012, 122: 92-105.

[210] BROWN J F, TOLLERUD H J, BARBER C P, et al. Lessons learned implementing an operational continuous United States national land change monitoring capability: the Land Change Monitoring, Assessment, and Projection (LCMAP) approach[J]. Remote Sensing of Environment, 2020, 238: 111356.

[211] STEHMAN S V, PENGRA B W, HORTON J A, et al. Validation of the U.S. geological survey's land change monitoring, assessment and projection collection 1.0 annual land cover products 1985—2017[J]. Remote Sensing of Environment, 2021, 265: 112646.

[212] HANSEN M C, DEFRIES R S, TOWNSHEND J R G, et al. Global percent tree cover at a spatial resolution of 500 meters: first results of the MODIS vegetation continuous fields algorithm[J]. Earth Interactions, 2003, 7(10): 1-15.

[213] SEXTON J O, NOOJIPADY P, ANAND A, et al. A model for the propagation of uncertainty from continuous estimates of tree cover to categorical forest cover and change[J]. Remote Sensing of Environment, 2015, 156: 418-425.

[214] HIRSCHMUGL M, DEUTSCHER J, SOBE C, et al. Use of SAR and optical time series for tropical forest disturbance mapping[J]. Remote Sensing, 2020, 12(4): 727.

[215] SHIMIZU K, OTA T, MIZOUE N. Detecting forest changes using dense landsat 8 and Sentinel-1 time series data in trop-

ical seasonal forests [J]. Remote Sensing, 2019, 11(16): 1899.

[216] REICHE J, DE BRUIN S, HOEKMAN D, et al. A Bayesian approach to combine landsat and ALOS PALSAR time series for near real-time deforestation detection [J]. Remote Sensing, 2015, 7(5): 4973-4996.

[217] REICHE J, VERBESSELT J, HOEKMAN D, et al. Fusing Landsat and SAR time series to detect deforestation in the tropics[J]. Remote Sensing of Environment, 2015, 156: 276-293.

[218] SHEN Wenjuan, LI Mingshi, HUANG Chengquan, et al. Mapping annual forest change due to afforestation in Guangdong province of China using active and passive remote sensing data[J]. Remote Sensing, 2019, 11(5): 490.

[219] SHEN Wenjuan, LI Mingshi, HUANG Chengquan, et al. Annual forest aboveground biomass changes mapped using ICESat/GLAS measurements, historical inventory data, and time-series optical and radar imagery for Guangdong province, China[J]. Agricultural and Forest Meteorology, 2018, 259: 23-38.

[220] SHEN Wenjuan, LI Mingshi, HUANG Chengquan, et al. Quantifying live aboveground biomass and forest disturbance of mountainous natural and plantation forests in Northern Guangdong, China, based on multi-temporal landsat, PALSAR and field plot data[J]. Remote Sensing, 2016, 8(7): 595.

[221] HAYASHI M, MOTOHKA T, SAWADA Y. Aboveground biomass mapping using ALOS-2/PALSAR-2 time-series images for Borneo's Forest[J]. IEEE Journal of Selected Topics in Applied Earth Observations and Remote Sensing, 2019, 12(12): 5167-5177.

[222] ZHAO Feng, SUN Rui, ZHONG Liheng, et al. Monthly mapping of forest harvesting using dense time series Sentinel-1 SAR imagery and deep learning[J]. Remote Sensing of Environment, 2022, 269: 112822.

[223] REICHE J, MULLISSA A, SLAGTER B, et al. Forest disturbance alerts for the Congo Basin using Sentinel-1[J]. Environmental Research Letters, 2021, 16(2): 024005.

[224] SCHROEDER T A, WULDER M A, HEALEY S P, et al. Mapping wildfire and clearcut harvest disturbances in boreal forests with Landsat time series data[J]. Remote Sensing of Environment, 2011, 115(6): 1421-1433.

[225] ZHAO Feng, HUANG Chengquan, ZHU Zhiliang. Use of vegetation change tracker and support vector machine to map disturbance types in greater yellowstone ecosystems in a 1984—2010 landsat time series[J]. IEEE Geoscience and Remote Sensing Letters, 2015, 12(8): 1650-1654.

[226] SCHROEDER T A, SCHLEEWEIS K G, MOISEN G G, et al. Testing a Landsat-based approach for mapping disturbance causality in U. S. forests [J]. Remote Sensing of Environment, 2017, 195: 230-243.

[227] SCHLEEWEIS K G, MOISEN G G, SCHROEDER T A, et al. US national maps attributing forest change: 1986—2010[J]. Forests, 2020, 11(6): 653.

[228] HERMOSILLA T, WULDER M A, WHITE J C, et al. Regional detection, characterization, and attribution of annual forest change from 1984 to 2012 using Landsat-derived time-series metrics[J]. Remote Sensing of Environment, 2015, 170: 121-132.

[229] WHITE J C, WULDER M A, HERMOSILLA T, et al. A nationwide annual characterization of 25 years of forest disturbance and recovery for Canada using Landsat time series [J]. Remote Sensing of Environment, 2017, 194: 303-321.

[230] SENF C, SEIDL R. Mapping the forest disturbance regimes of Europe[J]. Nature Sustainability, 2021, 4(1): 63-70.

[231] CHEN Xuexia, VOGELMANN J E, ROLLINS M, et al. Detecting post-fire burn severity and vegetation recovery using multitemporal remote sensing spectral indices and field-collected composite burn index data in a ponderosa pine forest[J]. International Journal of Remote Sensing, 2011, 32(23): 7905-7927.

[232] SOVEREL N O, PERRAKIS D D B, COOPS N C. Estimating burn severity from Landsat dNBR and RdNBR indices across western Canada[J]. Remote Sensing of Environment, 2010, 114(9): 1896-1909.

[233] TAO Xin, HUANG Chengquan, ZHAO Feng, et al. Mapping forest disturbance intensity in North and South Carolina using annual Landsat observations and field inventory data[J]. Remote Sensing of Environment, 2019, 221: 351-362.

[234] SKOG K E, NICHOLSON G A. Carbon cycling through wood products: the role of wood and paper products in carbon sequestration[J]. Forest Products Journal, 1998, 48(7-8): 75-83.

[235] WOODBURY P B, SMITH J E, HEATH L S. Carbon sequestration in the U.S. forest sector from 1990 to 2010[J]. Forest Ecology and Management, 2007, 241(1-3): 14-27.

[236] JOHNSON T G. United States timber industry—an assessment of timber product output and use, 1996[R]. Asheville, NC: U.S. Department of Agriculture, Forest Service, Southern Research Station, 2001.

[237] ZHU Zhiliang, BERGAMASCHI B, BERNKNOPF R, et al. A method for assessing carbon stocks, carbon sequestration, and greenhouse-gas fluxes in ecosystems of the United States under present conditions and future scenarios[R]. Reston, VA: US Geological Survey, 2010.

[238] LING P Y, BAIOCCHI G, HUANG Chengquan. Estimating annual influx of carbon to harvested wood products linked to forest management activities using remote sensing [J]. Climatic Change, 2016, 134(1-2): 45-58.

[239] ROSEN A, KUMAR R. NASA-ISRO SAR (NISAR) Mission Status [C] // Proceedings of the 2021 IEEE Radar Conference (RadarConf21). Atlanta, USA: IEEE. 2021.

[240] QUEGAN S, LE TOAN T, CHAVE J, et al. The European Space Agency BIOMASS mission: measuring forest above-

ground biomass from space[J]. Remote Sensing of Environment, 2019, 227: 44-60.

[241] LE TOAN T, QUEGAN S, DAVIDSON M W J, et al. The BIOMASS mission: mapping global forest biomass to better understand the terrestrial carbon cycle[J]. Remote Sensing of Environment, 2011, 115(11): 2850-2860.

[242] PULLIAINEN J T, KURVONEN L, HALLIKAINEN M T. Multitemporal behavior of L- and C-band SAR observations of boreal forests[J]. IEEE Transactions on Geoscience and Remote Sensing, 1999, 37(2): 927-937.

[243] MAHDIANPARI M, SALEHI B, MOHAMMADIMANESH F, et al. Random forest wetland classification using ALOS-2 L-band, RADARSAT-2 C-band, and TerraSAR-X imagery [J]. ISPRS Journal of Photogrammetry and Remote Sensing, 2017, 130: 13-31.

[244] HUANG Xiaodong, ZINITI B, TORBICK N, et al. Assessment of forest above ground biomass estimation using multi-temporal C-band Sentinel-1 and polarimetric L-band PALSAR-2 data[J]. Remote Sensing, 2018, 10(9): 1424.

[245] MITCHELL A L, TAPLEY I, MILNE A K, et al. C- and L-band SAR interoperability: filling the gaps in continuous forest cover mapping in Tasmania[J]. Remote Sensing of Environment, 2014, 155: 58-68.

[246] CHAVE J, RÉJOU-MÉCHAIN M, BÚRQUEZ A, et al. Improved allometric models to estimate the aboveground biomass of tropical trees[J]. Global Change Biology, 2014, 20(10): 3177-3190.

[247] HO TONG MINH D, NGO Y N, LÊ T T. Potential of P-Band SAR tomography in forest type classification[J]. Remote Sensing, 2021, 13(4): 696.

[248] RANSON K J, SUN Guoqing. Northern forest classification using temporal multifrequency and multipolarimetric SAR images[J]. Remote Sensing of Environment, 1994, 47(2): 142-153.

[249] WOLTER P T, TOWNSEND P A. Multi-sensor data fusion for estimating forest species composition and abundance in northern Minnesota[J]. Remote Sensing of Environment, 2011, 115(2): 671-691.

[250] ERINJERY J J, SINGH M, KENT T. Mapping and assessment of vegetation types in the tropical rainforests of the Western Ghats using multispectral Sentinel-2 and SAR Sentinel-1 satellite imagery[J]. Remote Sensing of Environment, 2018, 216: 345-354.

[251] LIU Yanan, GONG Weishu, HU Xiangyun, et al. Forest type identification with random forest using Sentinel-1A, Sentinel-2A, multi-temporal Landsat-8 and DEM data[J]. Remote Sensing, 2018, 10(6): 946.

[252] YU Ying, LI Mingzw, FU Yu. Forest type identification by random forest classification combined with SPOT and multi-temporal SAR data[J]. Journal of Forestry Research, 2018, 29(5): 1407-1414.

[253] MERONI M, D'ANDRIMONT R, VRIELING A, et al. Comparing land surface phenology of major European crops as derived from SAR and multispectral data of Sentinel-1 and -2[J]. Remote Sensing of Environment, 2021, 253: 112232.

[254] WANG Hongquan, MAGAGI R, GOÏTA K, et al. Crop phenology retrieval via polarimetric SAR decomposition and random forest algorithm[J]. Remote Sensing of Environment, 2019, 231: 111234.

[255] TRAN A T, NGUYEN K A, LIOU Y A, et al. Classification and observed seasonal phenology of broadleaf deciduous forests in a tropical region by using multitemporal Sentinel-1A and Landsat 8 data[J]. Forests, 2021, 12(2): 235.

[256] FRISON P L, FRUNEAU B, KMIHA S, et al. Potential of Sentinel-1 data for monitoring temperate mixed forest phenology[J]. Remote Sensing, 2018, 10(12): 2049.

[257] LEFSKY M A, HUDAK A T, COHEN W B, et al. Geographic variability in lidar predictions of forest stand structure in the Pacific Northwest[J]. Remote Sensing of Environment, 2005, 95(4): 532-548.

[258] SUN G, RANSON K J, KIMES D S, et al. Forest vertical structure from GLAS: an evaluation using LVIS and SRTM data[J]. Remote Sensing of Environment, 2008, 112(1): 107-117.

[259] TANG H, GANGULY S, ZHANG G, et al. Characterizing leaf area index (LAI) and vertical foliage profile (VFP) over the United States[J]. Biogeosciences, 2016, 13(1): 239-252.

[260] ZOLKOS S G, GOETZ S J, DUBAYAH R. A meta-analysis of terrestrial aboveground biomass estimation using lidar remote sensing[J]. Remote Sensing of Environment, 2013, 128: 289-298.

[261] PANG Yong, LI Zengyuan, JU Hongbo, et al. LiCHy: The CAF's LiDAR, CCD and hyperspectral integrated airborne observation system[J]. Remote Sensing, 2016, 8(5): 398.

[262] LU Jiaming, HUANG Chengquan, TAO Xin, et al. Annual forest disturbance intensity mapped using Landsat time series and field inventory data for the conterminous United States (1986—2015)[J]. Remote Sensing of Environment, 2022, 275: 113003.

[263] SHEFFIELD R M, THOMPSON M T. Hurricane Hugo effects on South Carolina's forest resource[R]. Asheville, NC: U. S. Department of Agriculture, Forest Service, Southeastern Forest Experiment Station, 1992.

[264] CHAMBERS J Q, FISHER J I, ZENG Hongcheng, et al. Hurricane Katrina's carbon footprint on U.S. gulf coast forests[J]. Science, 2007, 318(5853): 1107.

[265] HURTT G, ZHAO M, SAHAJPAL R, et al. Beyond MRV: high-resolution forest carbon modeling for climate mitigation planning over Maryland, USA[J]. Environmental Research Letters, 2019, 14(4): 045013.